Parametric Study on Flux Activated Tungsten Inert Gas Welding of AISI 316 and Duplex 2205 Steel

A dissertation submitted
in partial fulfillment of the requirements
for the degree of

Master of Engineering

in

CAD/ CAM Engineering

by

Sneh Pragya

Registration No.: 801381026

Under the Supervision of

Dr. Anirban Bhattacharya
Assistant Professor

Dr. Tarun Kumar Bera
Associate Professor

MECHANICAL ENGINEERING DEPARTMENT

THAPAR UNIVERSITY, PATIALA

July, 2015

CERTIFICATE

I hereby declare that the thesis entitled "**Parametric Study on Flux Activated Tungsten Inert Gas Welding of AISI 316 and Duplex 2205 Steel** " is an authentic record of my work carried out as requirements for the award of the degree of **Master of Engineering** in **CAD/CAM Engineering** at **Thapar University, Patiala** under the supervision of **Dr. Anirban Bhattacharya**, Assistant Professor, Mechanical Engineering Department and **Dr. Tarun Kumar Bera**, Associate Professor, Mechanical Engineering Department, Thapar University, Patiala during July, 2013 to July, 2015. No part of the matter embodied in this report has been submitted to any other university or institute for the award of any degree.

Date: 15/07/2015

Sneh Pragya

It is certified that the above statement made by the student is correct to the best of my/our knowledge and belief.

Anirban Bhattacharya 15/7/15

Dr. Anirban Bhattacharya
Assistant Professor
Mechanical Engineering Department
Thapar University, Patiala - 147004

Tarun Kumar Bera 15/7/15

Dr. Tarun Kumar Bera
Associate Professor
Mechanical Engineering Department
Thapar University, Patiala - 147004

Countersigned by

Head, Mechanical Engineering Department
Thapar University, Patiala – 147004

Dean of Academic Affairs
Thapar University, Patiala - 147004

Dedicated to

My dear loving Family and friend Naveen

Acknowledgements

With deep sense of gratitude I express my sincere thanks to my guide **Dr. Anirban Bhattacharya** and **Dr. Tarun Kumar Bera** for their valuable guidance, proper advice and constant encouragement during my work on this thesis.

I also feel very much obliged to **Dr. S. K. Mohapatra**, Professor and head of Mechanical Engineering department.

A very special thanks and reward to non–teaching staff members **Mr. M. Suri, Mr. Surinder, Mr. Rajinder, Mr. Narender,** of central Workshop, Thapar University, Patiala for their help during this period of work.

My very special Thanks go to all my family members. Their love, affection and patience made this work possible and the blessings and encouragement of my beloved parents and my brother greatly helped me in carrying out this research work. I am so thankful to my best friend **Naveen Mittal** for his lot of help and cooperation.

I am also wish to record my sincere thanks to the department for providing the financial support.

SNEH PRAGYA

Roll No.: 801381026

Abstract

Joining of thin plate (~ 2–3 mm) by Tungsten Inert Gas (TIG) welding gives satisfactory results in terms of depth of penetration but for relatively higher thickness plates the speed of welding should be reduced to achieve desired penetration that lowers productivity. So, to increase the depth of penetration at reasonable good welding speed some oxide powders are used. These oxide powders are mixed with acetone and are applied on the plate before welding. These oxide powders cause higher depth to width ratio and as a result of this the materials get joined through all its thickness properly. This process of TIG welding when oxide flux is used is called Activated TIG (ATIG) welding.

The purpose of this research work is to study the effects of specific fluxes used in the TIG welding on joint strength by analyzing impact strength, variation of microhardness and bending when two similar graded austenitic stainless steel plates are welded together. This process is repeated for two materials i.e. AISI 316 of 6 mm thickness and Duplex 2205 of 7 mm thickness. Plates were prepared with the edge groove at an angle of 45º. Filler rods with 3 mm diameter are made of AISI 316 and Duplex 2205. The torch was given a constant speed of 1.3 mm/s and constant height of 3 mm with the help of self made cart setup. There were three varying currents 125 A, 150 A and 175 A and three different gas flow rates 10 L/min, 13 L/min and 16 L/min with different torch angles 50º, 70º and 90º with the horizontal. Two different gases (pure Ar and Ar + 5% H_2) were used as protecting gases and three different oxide powders TiO_2, MoS_2 and SiO_2 mixed with acetone (flux) is applied on the steel plates before welding. After welding, toughness and bending test were carried out to study the mechanical strength of the joints. The results indicate that SiO_2 and TiO_2 fluxes lead to a significant increase in the depth penetration capability of TIG welds. The activated TIG process can increase the joint penetration and maximum bending load was found using SiO_2 flux with higher gas flow rate. Use of TiO_2 flux provided higher toughness of the welded joints. Higher bending load was achieved when Ar + H_2 is used as shielding gas as compared to pure Ar.

Key words: TIG; ATIG; Oxide; Flux; Toughness; Ductility; Microhardness; Microstructure.

Contents

List of Figures

List of Tables

Acronyms

AISI	American Iron and Steel Institute
ANOVA	Analysis of Variance
ATIG	Activated Tungsten Inert Gas
DF	Degree of Freedom
HAZ	Heat Affected Zone
HVN	Vickers Hardness Number
MS	Mean Square
SNR	Signal to Noise Ratio
SS	Sum of Square
TIG	Tungsten Inert Gas

Chapter 1

Introduction

1.1 Introduction

In our day to day life steel play very important role. When the corrosion less, long lasting better looking, ductile material is required for any product steel is used, for joining thinner metal sheets tungsten inert gas (TIG) welding is very famous; but a thicker plate cannot be welded in single pass and efficiency is reduced when welded with multi pass. To improve the quality of the TIG welding for thicker sheet oxide flux can be used. That method of TIG welding is called ATIG (activated TIG) in this thesis different types of fluxes are used with different combinations of parameters like current, gas flow rates and torch angles. Shielding gases affects the depth of penetration of the weld pool. Hydrogen increases thermal conductivity and fluidity so, it is mixed with the shielding gas argon. Different levels of all the parameters were selected to study the effect of flux and shielding gases. Higher current increases depth of penetration lower current increase the distortion. Higher gas flow rate constrict the arc which also increase the depth of penetration; lower gas flow rates minimizes the surface hardness because it does not cool the weld pool immediately. Higher torch angle constrict the arc as it direct enforce the weld pool; lower torch angle let arc spread on the parent material. In this experimental work different level of parameters and their effects are studied.

1.2 Welding

It is joining process for metals. It is obtained by heating to suitable temperature with or without use of filler metals and the filler metal has lower melting temperature than base metal; so, the joint gap is filled with either melt filler material or by the base metal itself after melting. In other word welding is used to metallurgical join two metal pieces together to produce; the process results in what is known as a permanent joint and the product is called weldment.

Welding is very old method to join materials. In middle age circular gold boxes were used to be made by pressure welding. Also hammering was the process to join the material specially irons. In 1890 the arc welding process with metal electrodes was invented. In 1900 coated metal electrode was invented in Great Britain. It was thin layer of clay on the electrode, and it helped to have stable arc. During 1885-1900 different resistance welding methods were developed like spot welding, flash butt welding, seam welding and projection welding.

First time automatic welding was used after the World War 1 in 1920. This was able to utilize bare electrode wire which was operated on direct current and utilized arc voltage by regulating the feed rate.

In 1920 the externally applied gases and shielding gases was started to be used. The concept for reasons of brittleness and porosity of welds due to presence of oxygen and nitrogen in contact with the molten weld pool was known. That time carbon electrodes were being used than tungsten electrodes were found preferable.

H.M. Hobart and P.K. Devers in 1926 first used argon and helium as shielding gases. It was used in gas tungsten arc welding process as well as gas metal arc welding. In 1930 the automatic processes for submerged arc welding were being used.

The welding gets started from a very simple joining process to the highly modified automated version now days. It is being used for different complex art purpose with precision by robots. It is used for every metallic products needed for day to day life. From the chair used to sit to the building which contains the chair [W.1].

1.3 Tungsten Inert Gas welding

This method of welding is quite famous for its high quality joints and clean welds. This is very efficient and precise process with less noise. During TIG welding very smooth arc is generated with very good weld pool. Approximately no spark or spatter is generated in this process and leaves very clean beads behind.

It is also called as gas tungsten arc welding. It is a welding process which joins metals by melting the metals to their melting point with an electric arc produced between the non

consumable tungsten electrode and the base metals to be weld. The inert gas is used as shielding to protect the arc and molten metal pool from contaminants in the atmosphere. The gas used is very inactive and protects the weld from oxidation and contamination from the atmosphere.

1.3.1 TIG setup

The TIG welding consists of a power source and an electrode which is the non-consumable tungsten rod, a gas cylinder and a paddle to release gas as required. Tungsten is a metal with a fusion point of more than 3300°C i.e. more than the double of the fusion point of metals which are usually being welded; so, it is used as the electrode. TIG welding also uses inert gas as shielding gas; inert gas does not combine with any other elements; so, used to protect the weld pool from the atmosphere. The arc is produced between the tungsten electrode and the weld. The filler material or filler rod is external and is introduced into the arc manually or through a wire feeder, filler material gets melt and fill the space between the two pieces to be welded.

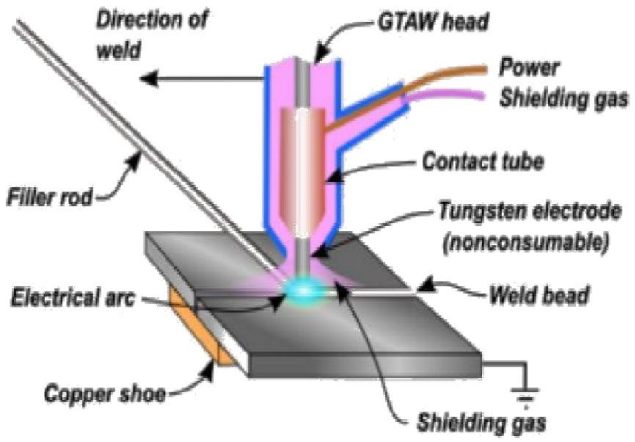

Figure 1.1: TIG welding [W.2]

1.3.2 Advantages and disadvantages of TIG

- TIG produces welds of great quality when used for thin sheets up to 2 mm.
- The TIG welds achieve very good appearance are as well as mechanically strength; so, it is the most preferred method for steels and other alloys.

- It is a better welding method because there is no spark, spatter or slag is produced during the process.
- Provides precise control of welding variables (i.e. heat and gas flow rates).
- When a thicker sheet more than 2 mm is to be welded tig welding cannot produce enough depth to width ratio in single pass. Welding efficiency decreases when multi pass of the TIG welding is done.
- Angular distortion and Surface hardening of the base metal occurs.

1.3.4 Applications

It is used for welding aluminum, magnesium, copper, nickel and its alloys, carbon alloys or stainless steels, Inconel, high temperature and hard surfacing alloys like zirconium and titanium. TIG welding is used for precision welding in atomic energy, aircraft, chemical and instrument industries, welding of sheet metal and thin sections.

1.4 Activated Tungsten Inert Gas welding

In this welding a thin layer of activated material (flux of oxides) is used on the base metal surface before TIG welding. This method of welding creates great effect on material strength. Oxide powders (of size ~30–60 μm) is mixed with acetone to a paint like consistency and applied a thin layer (~5–6 mg/cm^3) on the surface of base metal before TIG welding it. This method can provide higher penetration performance **(**~295**%)** than normal TIG welding. It also enhances the various mechanical properties like ductility and mechanical strength to the weld joint.

1.5 Marangoni effect

Active surface element such as oxygen or sulphur in the molten pool changes the fluid patterns by altering the surface tension gradient and these causes in a deep penetration or the flow of fluid toward higher surface tension from lower is called marangoni's effect.

For an example the tears of wine, surface tension decreases with alcohol concentration, and the surface tension is higher in the thin film than the bulk, the associated Marangoni stress drives up flow throughout the thin film, i.e. the wine climbs until reaching the top of the film, where it

accumulates in a band of fluid that thickens until eventually becoming gravitationally unstable and releasing the tears of wine.

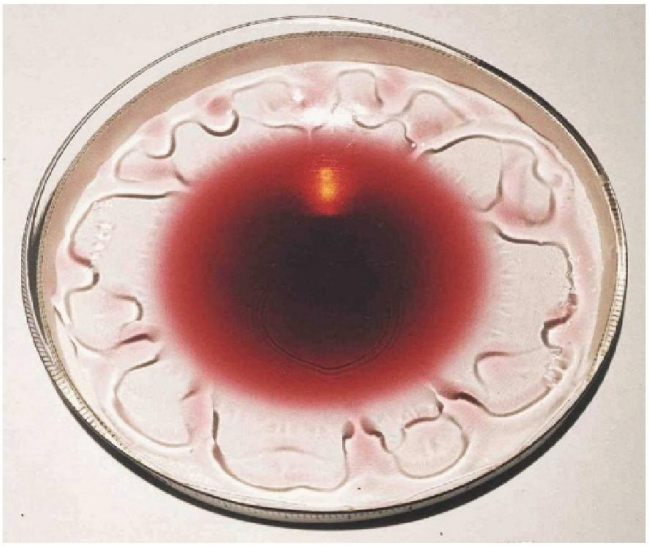

Figure 1.2: Tears of wine [W.3]

1.6 Welding of Austenitic and Duplex Stainless Steel

The properties of the weld joints in austenitic stainless steels get changed from the base metal because of precipitation, decomposition and segregation of material during solidification. These processes change the microstructure, which may affect the mechanical properties and the corrosion resistance. Weld joint properties varies from base metal. The microstructure changes, for duplex ferrite content in welded zone decreased during ATIG [Chern et al. 2011]. Welding consumables generally have a more austenitic composition with 2–4% more nickel than the parent steel for improved mechanical and corrosion.

It was also discovered that high currents increased the ferrites in welds and coarsened the microstructure. Deformation may occur at lower temperature. Duplex stainless steel produces more ferrite particles than the austenitic stainless steel.

1.7 Organization of the thesis

There are 5 chapters in this thesis. Here is the brief information about them all. Chapter 1 includes the introduction of welding its type. TIG welding and its advantages and disadvantage

with applications. It also contains the brief knowledge about activated TIG welding and its benefits. How marangony flow affects the welding mechanism is also described there.

Literature review is given in the Chapter 2; all the previous works have been done in this concern are explained there. Various developments in the TIG welding procedure and their results are discussed. Literature gap and objective of this area is also included in this chapter.

Chapter 3 explains all design of experiments and methods used in this thesis; it also explains the consumable materials. Chapter 4 has the major part of the thesis; it has all the result found in different tests performed. It also consists of the microscopic observation of all the weld joints.

Chapter 5 concludes the thesis.

Chapter 2

Literature Review

2.1 Introduction

This chapter contains the previous work done for the Effect of activated TIG welding on mechanical properties and microstructure. TIG welding was invented in 1923 since then many researches devoted their lives in quest to improve it. TIG welding has a big drawback when we try to weld thick steel plates. Many studies have been concluded in order to explore all the possible outcomes. Many different approaches are discussed in this chapter. Implications of different fluxes on materials with varying composition along with varying welding parameters have been discussed.

2.2 Review of literature

TIG welding is a very popular welding technique for high quality joints but limitation lies in the thickness of welding material. Many researches are being conducted to overcome this problem. Activated TIG showed many promising results. Result shows even a basic flux can increase depth up to 3 times but bead shape depends on individual flux. High electronegative elements attracts positively charged element outside the arc hence narrowing the arc [Modenesi et al. 2000].

Later it was found that activated flux change physical properties of weld pool. It was observed that the direction of surface tension around the area of welding pool is opposite between ATIG than conventional TIG and penetration for depth is closely related to oxygen content in weld pool. It caused surface tension gradients. When the oxygen content was in the range of 70-300ppm, ratio of depth to width increased to two times. TiO_2 was recommended for real world application because depth-width ratio is not dependent on quantity of TiO_2 flux and it also give good penetration results [Lu et al. 2002].

In 2003 Yang et al. [2003] found that penetration depth can be measured by monitoring the distribution of element Bismuth (Bi) in weldment. It was found that for good depth of penetration, combination of arc constriction with arc plasma constriction and surface tension gradient is required. Approx 53% increase in arc voltage was found which led to high heat density. When compared the fluxes SiO_2 and TiO_2 on material Stainless steel 0Cr18Ni9 with 6mm thickness It showed the molten metal flowed outward when flux used before welding.

Durgutlu [2003] compared different amount of H_2 in the mixture with pure Ar and suggested that 1.5% of H_2 with the Ar gives best result during the tensile test. Hardness was found lesser than the parent material. Penetration was found to be increasing with the amount of content of H_2.

Joining and welding research institute, Osaka University, Japan also studied the effect of Activated TIG welding on penetration-width ratio and verified arc contraction and fluid flows using various state of art technologies at their time. It was verified that flux such as SiO_2 and TiO_2 significantly increase penetration depth and sharp contraction of arc was observed at anode. Using x-ray transmission system out ward flow of fluids in conventional tig was observed whereas in activated tig flow was inward [Dong et al. 2004].

Xu et al. [2007] mentioned the penetration in the ATIG welding does not increase with the increase of content of flux above critical value. The weld pool penetration can be much larger when quantity of the flux is low; so, critical value for the quantity of flux is required to be achieved for the better depth of penetration in the weld pool.

Shyu et al. [2007] found significant penetration depth using activated flux on stainless steel 304. When compared Al_2O_3 made penetration worse and generated more slag then conventional welding. CaO was neutral in the process. Weldment of ATIG showed better mechanical properties then conventional. Delta ferrite content of stainless steel welds was more than conventional which are good in reducing cracking susceptibility.

SiO_2 was added with water and used as the flux and coating thickness was controlled by this method. It was mentioned that coating layer thickness must not exceed 200 μm. It was also mentioned the optimum layer thick was approx 40–70 μm as at optimum thickness more depth of penetration can be achieved [Ruckert et al. 2007].

Loureiro et al. [2008] in University of Columbia worked on effects of activated flux and shielding gas during TIG welding on microstructure when joined austenitic stainless steel, found that Flux causes small refinements in the steel welds microstructure in presence of Ar shield welding gases. It was also discovered that high currents increased the ferrites in welds and coarsened the microstructure. The amount of ferrite was not similar in welding joints made by using flux, contentment of ferrite was higher in central of welding joint then top of the same.

Tsann et al. [2011] studied the characteristics of duplex stainless steel in the national Taiwan University of science and technology Taipei found effects of flux on mechanical properties and microstructure when welding 6mm thick duplex stainless steel. Compared with conventional TIG welding, significant increase in mechanical strength and penetration capabilities were noted when fluxes SiO_2, MoO_3 and Cr_2O_3 were used. Activated TIG welding increased the current density at weld which increased the heat input. As a result ferrite content of the duplex 2205 stainless steel was decreased in the process.

It is found that maximum cathode jet velocity in case of 2% ThO_2-W cathode was 497m/s, in case of pure W cathode was only 156 m/s because of low current density caused by flatten surface heat transport at weld pool radiate outward decreases because of less velocity [Tasuku et al. 2011].

Niagaj et al. [2011] concluded in their studies on deformation of austenitic steel components found that Activated TIG had five times lesser angular distortion then conventional TIG welding and size of these distortions increase with width of steel plates. As a result deformation occurring during activated flux was four times lower when welding pipe connectors into plate of austenitic stainless steel.

Institute of metal research suggested that oxygen level within molten pool can be directly affected by the changes made in welding parameters of the TIG welding and this causes effect in temperature too. The Marangoni convention's strength and pattern is determined by oxygen level and heat generated in the molten pool. The pure He shielding gas in TIG process causes increase in oxygen content and outward Marangoni convection gets weakened results higher depth-width ratio [Dongjie et al. 2012].

Katherasan et al. [2012] used different mixture of shielding gases like pure Ar, Ar + CO_2(5%), Ar + CO_2(10%), Ar + CO_2(20%), Ar + CO_2(23%), Ar + CO_2(25%), and pure Carbon. When amount of CO_2 was increased it was found that ferrite content was less weld joint and also the joint had good ductility and toughness decreased.

Tseng et al. [2012] compared some ferric powders FeF_2, FeO and FeS, as Flux for activated TIG welding and stated FeF_2 had good surface looks than other ones. FeS caused an uncut into the weld. FeO and FeS caused good depth of penetration.

10mm thick steel plate was successfully welded by ATIG welding using by double side welding method. It was found that size of the grain become coarser then the parent material and hardness reaches to 420 HVN. When tested for tensile strength it was found the specimen fails at the parent material shows that the ATIG joint formed stronger joint than the parent material [Vasantharaja et al. 2013].

Amudarasan et al. [2013] researched for effect of filler material and stated that the weld joint formed by Austenitic Stainless Steel filler material shows higher toughness by 20% when compared with the same formed by Duplex Stainless Steel. It was also mentioned that the austenitic fillers showed more ductility than the duplex stainless steel filler wires.

Arunkumar et al. [2013] worked to increase depth of penetration in single pass by ATIG welding. 100% penetration was noted the constriction of arc due to flux. The tensile testing of weld samples showed that ATIG weld joint was more tensile than parent metal. No degradation of mechanical properties and mechanical properties was found in ATIG welding joints when compared with conventional TIG weld joints.

It has been found that by using ATIG also welding cracking susceptibility is reduced because of flux's property of current enhancement. Addition of nitrogen in argon shield gas can increase tensile strength, penetration depth [Huang et al. 2014].

DevaKumar et al. [2014] advised that to keep the heat low when welding AISI 304 stainless steel using TIG process because grain coarsening is less keeping good tensile strength and ductility. Joint strength in case of TIG is 20% more than gas metal arc welding and 10% more than

SMAW. Bowing distortion increases with increase in current because of increment in penetration.

Duhan et al. [2014] compared different flux and the mechanical properties formed with them. It was found MnO_2 increases more hardness of the fusion zone in the welded joints when compared with $MgCl_2$, ZnO and Fe_2O_3.

It was found in an experiment on UNS 31603 stainless steel. Nano particle oxide powder were mixed with water or methanol and produce more homogeneous solution then micro particle oxide which can then be easily implemented on metal surface. ATIG welding using nano particle SiO_2 flux can produce penetration depth of 5.24 times then convention TIG welding where as nano particle flux of Al_2O_3 does not give satisfactory results. Nano particle SiO_2 flux reduced angular distortion by 78% compared with conventional TIG [Tseng et al. 2014].

2.3 Summary of literature review

TIG welding is popular for producing high quality joints on stainless steel and the only drawback is it is not practical to weld very thick steel plates with this method. In the quest to find solution activated flux has shown significant results.

Researchers found 2-5 times increase in depth-width ratio, improvement in strength, toughness and microstructure. The factors and principles working in the process are believed to be arc plasma constriction and Marangoni effect. During welding release of oxygen in weld pool is the key reason for sudden change in the surface tension of the pool.

This change in surface tension cause inward flaw of material which cause depth of penetration. Many research has found SiO_2 and TiO_2 giving significant results. It has also been observed that shielding gas also its effect on weld pool. Mixture of some other gases like H_2 or CO_2 into pure Argon helps to increase in depth of penetration and add some more efficiency to the mechanical properties of the weld joint.

2.4 Scope and objectives of the present work

Based on the literature review and summery of literature review, the following objectives are decided for the present work.

- To study the effect of different activated flux (oxide and sulphide based) on mechanical strength of welded joints for austenitic and duplex stainless steels.
- To study the effect of shielding gas on mechanical properties (like bending load, toughness) during flux activated TIG welding. Commercially available pure Ar and Ar+H_2 (5% H_2) has been used for their purpose.
- To carry out a parametric study in order to identify the role of process parameters like fluxes, shielding gas, current, gas flow rate, torch angle on mechanical properties of joint prepared by ATIG welding.
- To study the effect of above process parameters on microhardness variation at fusion zone, heat affected zone (HAZ) of ATIG welding joints.
- Metallurgical characterization of fusion and HAZ are also carried out after ATIG welding for AISI316 and Duplex 2205 stainless steels.

Chapter 3

Materials and Methodology

3.1 Introduction

In this chapter all the details of materials and the machines used to create desired samples for different experiments are discussed. Selection of experimental parameters and their levels are based on pilot studies performed earlier. This chapter also includes setups of all the measuring machines to measure bending loads, toughness and micro hardness even the material composition.

3.2 Materials and consumables

There are many materials which got consumed during this study. Those are filler wires, work piece materials, shielding gases and oxide powders.

3.2.1 Work piece materials

In this study following materials are used:

AISI 316

Application list of AISI 316 is very wide in industrial area due to austenitic nature of it. It has several elements in its composition. Mostly it contains Cr 16-26% and Ni 8-24% which define its properties as non corrosive and higher toughness even at higher temperature. So for exact evaluation of each contain the material was tested in spectroscopy machine shown in Fig. 3.1

Figure 3.1: Spectroscopy machine

and result was found is mentioned in Table 3.1 which explains the average of element content found in three burns during the test. The result explains that the material has very less amount of carbon in it. Spectroscopic samples of material AISI 316 in Fig. 3.2.

Table 3.1: Spectroscopic result of AISI 316

Element	Test 1 (%)	Test 2 (%)	Test 3 (%)	Average (%)
Fe	68.4	68.1	68.2	68.2
C	0.0056	0.0050	0.0055	0.005
Si	0.210	0.210	0.215	0.212
Mn	1.27	1.28	1.28	1.28
P	0.0534	0.0571	0.059	0.0565
S	0.0124	0.0127	0.0131	0.0127
Cr	16.8	16.9	16.9	16.8
Mo	2.09	2.04	2.04	2.06
Ni	10.2	10.4	10.2	10.3
Al	0.0234	0.0625	0.005	0.0299
Co	0.279	0.282	0.274	0.278
Cu	0.389	0.387	0.403	0.393
Nb	0.0318	0.0337	0.0318	0.0324
Ti	0.0013	0.002	0.001	0.0014
V	0.0816	0.0815	0.0811	0.0814
W	0.0269	0.0520	0.0635	0.0475
Pb	0.0500	0.05	0.05	0.05

Figure 3.2: Spectroscopic samples of material AISI 316

Duplex 2205

This stainless steel contains both kinds of properties austenitic as well as ferrite this is why it is called duplex. The material has good corrosive resistance, good strength and formability.

It has more chromium than austenitic stainless steels and this makes it more corrosive resistant. It mostly contains Cr upto 23-24%. Table 3.2 explains all the contents of second material being used in this study.

Table 3.2: Spectroscopic result of Duplex 2205

Element	Test 1 (%)	Test 2 (%)	Test 3 (%)	Average (%)
Fe	65.8	66.5	66.2	66.2
C	< 0.0050	< 0.005	<0.005	<0.005
Si	0.273	0.246	0.264	0.261
Mn	1.65	1.66	1.66	1.66
P	0.0389	0.0399	0.0409	0.0399
S	<0.005	<0.005	<0.005	<0.005
Cr	23.4	22.7	22.9	23.0
Mo	3.45	3.39	3.50	3.45
Ni	4.78	4.91	4.84	4.84
Al	<0.001	<0.001	<0.001	<0.001
Co	0.105	0.1	0.102	0.102
Cu	0.214	0.216	0.222	0.217
Nb	0.0039	0.0045	0.0067	0.005
Ti	0.0106	0.0103	0.0109	0.06
V	0.120	0.117	0.117	0.118
W	<0.02	0.0223	<0.2	<0.02

Figure 3.3: Spectroscopic samples of Duplex 2205

3.2.2 Filler Wires

In TIG welding Filler wire is optional welding joint can be made with or without filler wire. In this study the base metal had groove of approx 3 mm of an angle of 90º; so, fillers were used to fill the grooves during welding process. Two different filler wires of diameter 3mm were chosen AISI 316 wire for AISI 316 and Duplex 2205 wire for Duplex 2205. The feed of filler wire also plays a major role in making weld beads after filling the groove. A continuous feed was maintained during the welding.

Figure 3.4: Duplex 2205 and AISI 316 Filler Wires

3.2.3 Shielding Gas

Shielding gas as name suggested are used to shield weld pool formed during welding and the electrode from oxygen and water vapors. For this purpose inert and semi-inert gasses are used. Gasses used in this experiment are Ar and combination of Ar and H_2. Wrong choice of shielding gas can lead porous and weak welds and scattered metal drops over the material. Useful properties of inert gasses like thermal conductivity and ease of ionization supports the welding process. So, in this study two types if shielding gas was used pure Ar and Ar + 5%H_2.

Figure 3.5: Argon gas cylinder with pressure and gas flow rate regulator

Argon is heavier then air which make it cover the welding surface and hence resist the air whereas hydrogen is lighter than air but has other properties like thermal conductivity. Gas flow rate influences other parameters like arc forming; weld pools shape and cooling rate of material and tungsten electrode. Hydrogen improves the molten metal's fluidity.

3.2.4 Activated flux

Activating flux is prepared using these component oxides and sulfide TiO_2, MoS_2 and SiO_2 packed in powdered form and of about 30–60 lm particle size. These oxide and sulfide powders are mixed with acetone to produce a paint-like consistency shown in Fig. 3.6. A thin layer of 0.02 mm thick flux is applied on the surface of the joint to be welded. The coating density of flux was approx 3–5 mg/cm². Fig. 3.7 shows the method used of applying flux on the workspace in the groove.

Figure 3.6: Consistency of flux

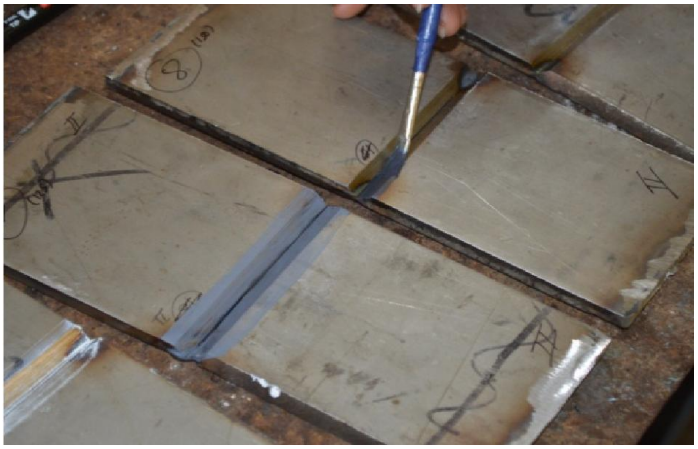

Figure 3.7: Application of flux

3.3 TIG welding setup

In this study TIG welding was done on tungsten inert gas welding manufactured by Techno weld. The arc current range is 0–500 A. The function of this machine is to produce arc between electrode and the work piece material. The arc produced generates ample of heat and that heat causes work piece material to melt. A parallel gas pipe is used to supply shielding gas to the weld pool made by molten metal to protect it from atmospheric contamination. A welding joint can be made either by filler wire or without that. In this machine filler was fed manually. Fig. 3.8 shows the TIG welding setup used in this process.

Figure 3.8: Welding machine

Figure 3.9: Welding cart with the nozzle.

According to requirement of steady movement of torch for smooth joint a cart was made. This cart helped in maintaining the torch in required vertical height from the work piece material. It also helped the torch to be moved in straight horizontal with minimal vibration on the smooth tracks of aluminium brackets. The setup was created to align torch properly in required inclination of 50º, 70º and 90º as shown in Fig.3.9.

3.4 Design of Experiments

Design of Experiments is the important part of any research. When number of parameters are more; larger no of trials are required; so, that every parameter can be studies. Minimising those trials becomes important. There are several methods, among them in this study Taguchi Experimental methods is used. This method is very efficient to determine the optimum result of any experimental study. Taguchi method plays an important role in selecting the most significant

factors among all. According to literature review TiO_2, SiO_2 and MoS_2 are best fluxes among the wide variety of oxide fluxes. So, these fluxes were selected similarly in case of shielding gas, current, gas flow rates and torch angles affect the weld joint properties. Thus these parameters were analysed with the Taguchi experimental method using L_{18} orthogonal array design.

3.4.1 Pilot Experimentation

For the pilot study five fluxes were chosen they were mixed with the combination of $^5C_2$. This combination brought 10 samples to be weld at constant current 120 A and gas flow rate 13 L/min.

Table 3.3: The combination set of samples

Experiment no.	Current (A)	Gas flow rate (L/min)	Flux mixture
1	120	13	TiO_2+ MnO_2
2	120	13	TiO_2+ SiO_2
3	120	13	TiO_2+ MoO_3
4	120	13	TiO_2+ Cr_2O_3
5	120	13	MnO_2+ SiO_2
6	120	13	MnO_2+ MoO_3
7	120	13	MnO_2+ Cr_2O_3
8	120	13	SiO_2+ MoO_3
9	120	13	SiO_2+ Cr_2O_3
10	120	13	MoO_2+ Cr_2O_3

Table 3.4: Result of TIG welding during Pilot studies

TIG welding witout flux

TIG welding with flux of oxides TiO_2+ MnO_2

TIG welding with flux of oxides TiO_2+ SiO_2

TIG welding with flux of oxides TiO_2+ MoO_3

TIG welding with flux of oxides TiO_2+ Cr_2O_3

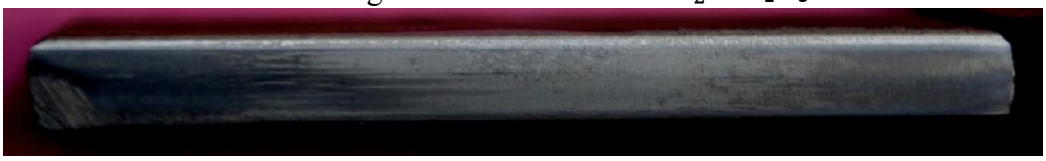

TIG welding with flux of oxides MnO_2+ SiO_2

TIG welding with flux of oxides MnO_2+ MoO_3

TIG welding with flux of oxides MnO_2+ Cr_2O_3

TIG welding with flux of oxides SiO_2+ MoO_3

TIG welding with flux of oxides SiO_2+ Cr_2O_3

TIG welding with flux of oxides MoO_3+ Cr_2O_3

On the basis of visual analysis it was found that higher depth to width ratio was achieved using SiO_2+MoO_3 during the TIG Welding.

3.4.2 Selection of process parameters and their levels

All the factors are listed that were used in this study in Table 3.5.

Table 3.5: Parameters selected for this experimental research

Sl no	Parameters			
1	Gas type	Ar	$Ar + H_2$	
2	Flux type	SiO_2	TiO_2	MoS_2
3	Current (A)	125	150	175
4	Gas flow rate (L/min)	10	13	16
5	Torch angle(°)	50	70	90

3.4.3 Selection of orthogonal array

Orthogonal array achieved using L_{18} with five different factors including gas type, flux type, current levels, gas flow rates, and torch angles as shown in Table 3.6.

Table 3.6: Orthogonal array selected for both set of materials AISI 316 and Duplex 2205

Sl no.	Gas	Flux	Current (A)	Gas flow rate (L/min)	Torch angle (º)
1	Ar	SiO_2	125	10	50
2	Ar	SiO_2	150	13	70
3	Ar	SiO_2	175	16	90
4	Ar	TiO_2	125	10	70
5	Ar	TiO_2	150	13	90
6	Ar	TiO_2	175	16	50
7	Ar	MoS_2	125	13	50
8	Ar	MoS_2	150	16	70
9	Ar	MoS_2	175	10	90
10	$Ar+H_2$	SiO_2	125	16	90
11	$Ar+H_2$	SiO_2	150	10	50
12	$Ar+H_2$	SiO_2	175	13	70
13	$Ar+H_2$	TiO_2	125	13	90
14	$Ar+H_2$	TiO_2	150	16	50
15	$Ar+H_2$	TiO_2	175	10	70
16	$Ar+H_2$	MoS_2	125	16	70
17	$Ar+H_2$	MoS_2	150	10	90
18	$Ar+H_2$	MoS_2	175	13	50

3.5 Measurement setup and sample preparation

After the design of orthogonal parameter array samples were prepared. Fig. 3.10 shows a sample tacked on back side having a grove of 90° of 3 mm deep and 6 mm shallow. This sample is of total length of 200 mm and 85 mm wide and 6 mm thick AISI 316 and Duplex 2205 of 7 mm thick.

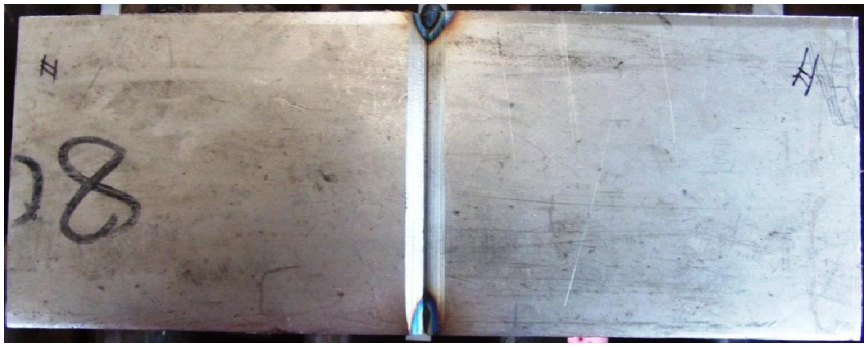

Figure 3.10: Sample with 90º groove

Before and after welding, samples were cleaned through buffing. In this process tinny metal wires as shown in Fig. 3.11 are used to brush the surface. Buffing cleans all the dust particles on the surface.

Figure 3.11: Buffing cleans all impurities before and after welding

3.5.1 Bending test

For bending steel plate upto 9.5 mm thick sample should be minimum 38 mm wide. So, total 18 samples were made of dimension 200 mm×38mm×6 mm for material AISI 316 and 18 for material Duplex 2205 of dimension 200 mm×38mm ×7 mm.

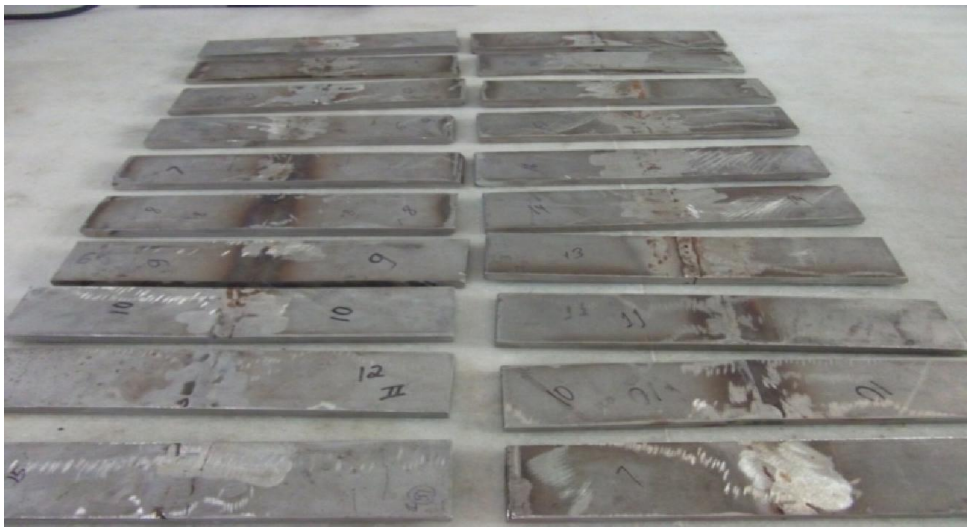

Figure 3.12: Bending samples

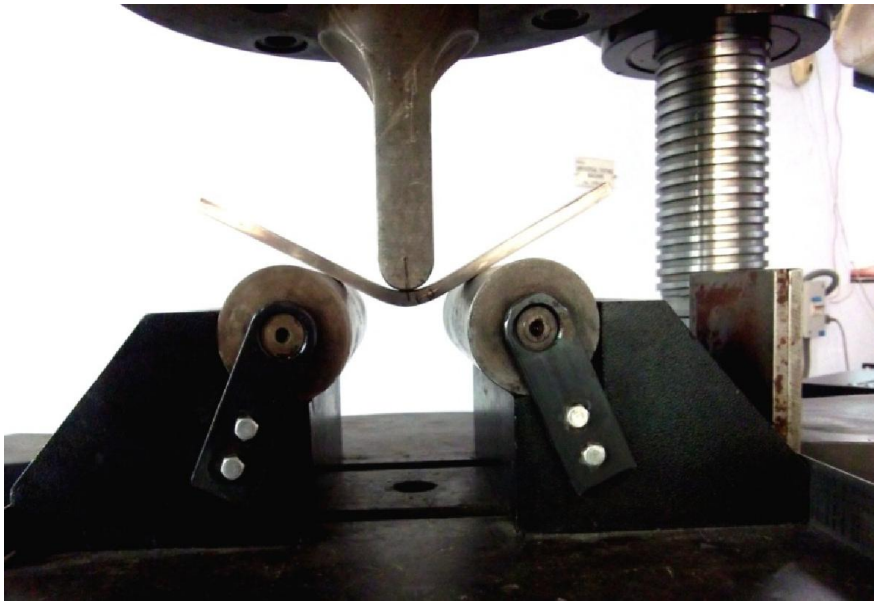

Figure 3.13: Bending machine setup

This is the bending machine setup. The gaps between the roller were kept 40 mm punch size was 24 mm in diameter and load was applied gradually. The capacity of this bending machine is 1000 kN.

3.5.2 Toughness Test

Charpy Impact test is used to evaluate the toughness. In this setup a pendulum is dropped from a certain height In this procedure is a mass is kept at an angle approx 135º -140º from vertical and fall from that height the with the energy 300 J and hit the specimen and again rise arrow to a new height .

Figure 3.14 Charpy cum Izod impact testing machine

There is some energy difference which is evaluated with difference of height achieved so this energy difference is the energy consumed by the specimen and that energy consumed by the specimen is called toughness. The machine used in this study has maximum toughness capacity is 300 J.

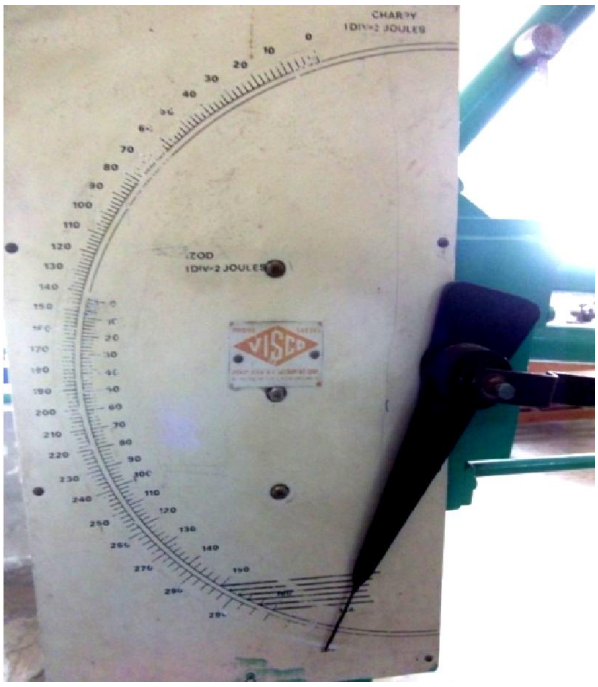

Figure 3.15 Charpy impact testing machines dial

In this study, 72 impact testing samples were made i.e. 36 for AISI 316 and 36 for Duplex 2205. The standard dimensions according to ASTM for impact is 10mm×10mm×55mm but in this 6mm and 7 mm thick plates are to be studied so the dimensions were chosen 10mm×6mm×55mm (AISI 316) and 10mm×7mm×55mm (Duplex 2205). As shown in Fig. 3.16 notches had been cut on each sample which was 2 mm deep and 45º in angle.

Figure 3.16 Sample with notch angle 45º

Figure 3.17: Samples prepared for impact test

3.5.3 Microhardness tester

Indentation hardness test tests microhardness by indenting its diamond indent on the surface of the specimen to be tested as shown in Fig. 3.18. Indenter dwells for 20 s into the work piece and then gets back to its position to make sure the plastic deformation. For steel microhardness of base material ranged approx 350 HVN; so, 300 gm is applied as load by indent. In this setup, 400X lenses are used to locate the interface zone of the fusion and HAZ in the weld samples. 3 indents were made in fusion zone near the interface and 3 indents were made in HAZ. This result is discussed in chapter 4.

Before this test samples were polished on polishing machine shown if Fig. 3.19. In this machine disc is mounted upon which emery papers can be fixed as required. These discs can rotate upto 1000 rpm, but these samples were polished below 600 rpm by different graded emery papers shown in Fig. 3.20.

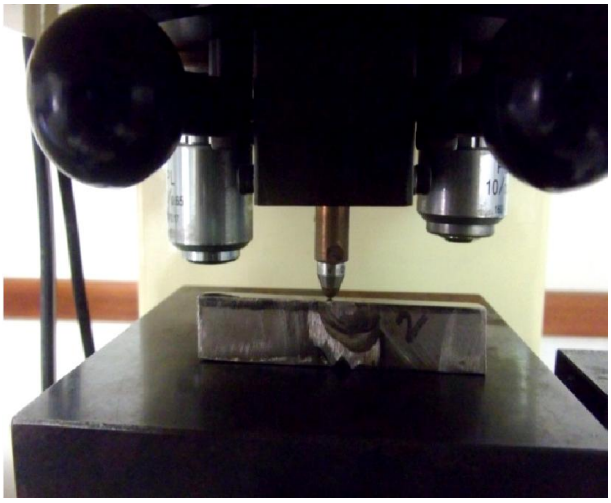

Figure 3.18: Indents on the samples for microhardness test

Figure 3.19: Polishing machine

Figure 3.20: Emery papers of different grades

3.5.4 Metallurgical microscope

Metallurgical microscope can be zoomed upto 1000X and make it visible to see each and every micro detail a material can have. 1000X is the limit of this microscope beside this it has three other different lenses in it 100X, 200X and 500X. In this study this microscope is used to view the interface zone of the weld's fusion zone and HAZ.

Figure 3.21: Metallurgical microscope

For making welding profile visible it needed to be polished properly with very fine graded emery papers P1000 followed by P2000. It is very necessary to remove every stain from the sample. After polished the samples are being etched by suitable etching agent. For AISI 316 and Duplex 2205 Carpenter was found suitable.

The composition of carpenter is mentioned in Table 3.7. The Carpenter looks like dark yellow as shown in Fig. 3.22 and had a very pungent smell.

Table 3.7: Composition of Carpenter

Content	Quantity
Ferric chloride	85 gm
Cupric chloride	2.4 gm
Alcohol	122 ml
Hydrochloride acid	122 ml
Nitric acid	6 ml

Figure 3.22: Etchant Carpenter

Chapter 4

Results and Discussions

4.1 Introduction

In this chapter all the analysis is mentioned including effect of welding parameters like flux, current, gas flow rate, torch angle and gas type for welding two materials AISI 316 and Duplex 2205. Different test result defines different things. In this study Taguchi experimental method is used. There are five factors and different results of bending test, impact test and microstructure. Results are analysed with the help of analysis of variance (ANOVA), Response Table, Main graph plots and ANOVA for SN ratios are explained. All result has been concluded with the significant parameters and contribution factors.

4.2 Bending test

Bending test is required to evaluate the maximum load sustained by the material before crack is initiated. For bending weld sample face bend teat is applied. This bend test is used to determine the ductility of fusion welds. The samples are machined approximately 38 mm wide, for at least 152 mm in length with the weld at the centre, and a gradual load is applied on the back of welded face.

4.2.1 Bend test analysis for AISI 316

The bending test result is mentioned in Table 4.1 it explains with the help of orthogonal array of L_{18} that which set of parameter resulted what.

Experiment no 10 has reached maximum bending load before the crack is 20.95 kN where parameters were chosen as gas type = Ar+H_2 flux = SiO_2, current = 125 A, Gas flow rate = 16 L/min and torch Angle = 90° on the other side experiment no 13 has lowest bending load = 5 kN this has parameters levels as Gas type = Ar+H_2, flux = TiO_2, current = 125 A, Gas flow rate = 13 L/min and torch angle = 90°.

Table 4.1: Maximum bend loads for AISI 316 samples

Sl no.	Gas	Flux	Current (A)	Gas flow rate(L/min)	Torch angle(°)	Maximum bend Load (kN)
1	Ar	SiO_2	125	10	50	11.65
2	Ar	SiO_2	150	13	70	8.90
3	Ar	SiO_2	175	16	90	9.70
4	Ar	TiO_2	125	10	70	13.50
5	Ar	TiO_2	150	13	90	12.20
6	Ar	TiO_2	175	16	50	11.85
7	Ar	MoS_2	125	13	50	12.20
8	Ar	MoS_2	150	16	70	9.55
9	Ar	MoS_2	175	10	90	12.95
10	Ar+H_2	SiO_2	125	16	90	20.20
11	Ar+H_2	SiO_2	150	10	50	12.25
12	Ar+H_2	SiO_2	175	13	70	13.10
13	Ar+H_2	TiO_2	125	13	90	5.00
14	Ar+H_2	TiO_2	150	16	50	10.50
15	Ar+H_2	TiO_2	175	10	70	6.20
16	Ar+H_2	MoS_2	125	16	70	10.85
17	Ar+H_2	MoS_2	150	10	90	12.30
18	Ar+H_2	MoS_2	175	13	50	13.70

The mean value of analysis of variance is given in Table 4.2 and it describes the significance of every factors.

The contribution percentage is also calculated to describe the different factors. Flux influence the welding by highest contribution then contribution of factor in sequence torch angle, current, gas flow rate and gas type was found.

Table 4.2: ANOVA for bending test of AISI 316

Source	DF	SS (Seq)	SS (Adj)	MS (Adj)	F value	P value
Gas type	1	0.142	0.142	0.1422	0.01	0.928
Flux type	2	24.625	24.625	12.3126	0.75	0.501
Current (A)	2	5.408	5.408	2.7039	0.17	0.850
Gas Flow rate (L/min)	2	4.750	4.750	2.3751	0.15	0.867
Torch angle (º)	2	11.450	11.450	5.7251	0.35	0.715
Residual Error	8	130.700	130.700	16.3375		
Total	17	177.076				

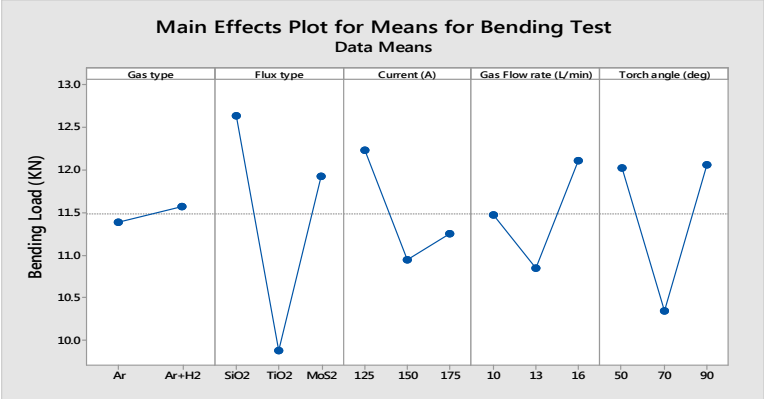

Figure 4.1: Plot for bending test of AISI 316

Figure 4.1 justifies the result mention above that , on X axis all the factors are set and on Y axis bending load (kN) is set and the result shows that flux with SiO_2 affects the most the bending load i.e. SiO_2 increases the bending load. TiO_2 is found to be decreasing it. MoS_2 is found to nominal in this case. When gas type is compared Ar +H_2 found to be leading factor than pure Ar. Reason can be considers for this is H_2 increase the fluidity of the molten pool and helps in getting higher penetration .when current is compared 125 A lead the influence when applied with fluxes SiO_2 TiO_2 and MoS_2. Similarly in case of gas flow rates 16L/min reasons for the ductility, 10L/min responded average and 13 L/min was found low efficient gas rate or the process. In case of torch angle torch 50º and 90º almost respond similar but 70º respond less efficiently.

Table 4.3: Response for bending test of AISI 316

Level	Gas type	Flux type	Current(A)	Gas Flow rate (L/min)	Torch angle(°)
1	11.389	12.633	12.233	11.475	12.025
2	11.567	9.875	10.950	10.850	10.350
3		11.925	11.250	12.108	12.058
Delta	0.178	2.758	1.283	1.258	1.708
Rank	5	1	3	4	2

Table 4.3 describes the responses of different parameters. This table also represent the rank of factors on the basis of delta values obtained. Here flux type has the highest delta value of 2.758 and gas type has the lowest delta value 0.178 similarly torch angle has 1.708, current has 1.283 and gas flow rate has 1.258 delta value.

Table 4.4: Bent samples of material AISI 316

Experiment No 1	Experiment No 2	Experiment No 3
		
Experiment No 4	Experiment No 5	Experiment No 6
		
Experiment No 7	Experiment No 8	Experiment No 9
		
Experiment No 10	Experiment No 11	Experiment No 12
	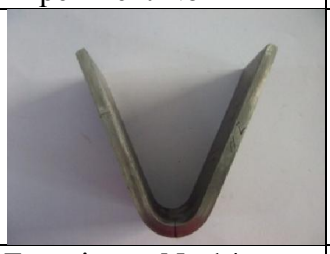	
Experiment No 13	Experiment No 14	Experiment No 15
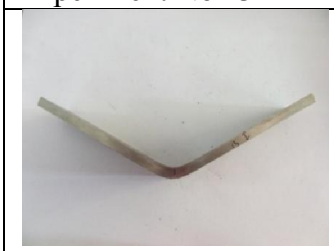		
Experiment No 16	Experiment No 17	Experiment No 18
	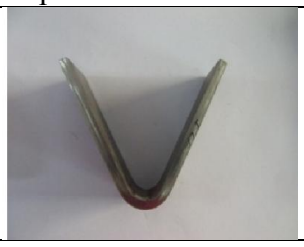	

4.2.2 Bend test analysis for Duplex 2205

In Table 4.5 bending test result has been explained. An orthogonal array of L_{18} samples explains the result caused by different parameters.

Experiment no 6 has reached maximum bending load before the cracking is 29.05 kN where parameters were chosen as gas type = Ar, flux = TiO_2, current = 175 A, Gas flow rate = 16 L/min and Torch Angle = 50° on the other side experiment no 8 has lowest bending load = 10 kN this has parameters levels as Gas type = Ar, flux = MoS_2, current = 150 A, Gas flow rate = 16 L/min and Torch Angle = 70°.

Table 4.5: Maximum bend loads for Duplex 2205 samples

Sl no.	Gas	Flux	Current (A)	Gas Flow rate (L/min)	Torch angle (°)	Maximum Bend Load kN
1	Ar	SiO_2	125	10	50	18.05
2	Ar	SiO_2	150	13	70	25.50
3	Ar	SiO_2	175	16	90	21.20
4	Ar	TiO_2	125	10	70	16.15
5	Ar	TiO_2	150	13	90	16.80
6	Ar	TiO_2	175	16	50	29.05
7	Ar	MoS_2	125	13	50	21.10
8	Ar	MoS_2	150	16	70	10.85
9	Ar	MoS_2	175	10	90	23.45
10	Ar+H_2	SiO_2	125	16	90	23.15
11	Ar+H_2	SiO_2	150	10	50	25.10
12	Ar+H_2	SiO_2	175	13	70	28.20
13	Ar+H_2	TiO_2	125	13	90	23.25
14	Ar+H_2	TiO_2	150	16	50	28.55
15	Ar+H_2	TiO_2	175	10	70	14.50
16	Ar+H_2	MoS_2	125	16	70	15.15
17	Ar+H_2	MoS_2	150	10	90	16.65
18	Ar+H_2	MoS_2	175	13	50	22.95

After applying ANOVA on the results it is found that torch angles is influencing the results most by contribution factor followed by flux type , gas flow rate, current and gas type in decreasing order.

Table 4.6: ANOVA for mean bending load of Duplex 2205

Source	DF	SS (Seq)	SS (Adj)	MS (Adj)	F value	P value
Gas type	1	13.09	13.09	13.09	0.55	0.481
Flux type	2	81.11	81.11	40.55	1.69	0.244
Current (A)	2	44.59	44.59	22.30	0.93	0.433
Gas Flow rate (L/min)	2	48.09	48.09	24.05	1.00	0.408
Torch angle (°)	2	99.95	99.95	49.98	2.09	0.186
Residual Error	8	191.55	191.55	23.94		
Total	17	478.38				

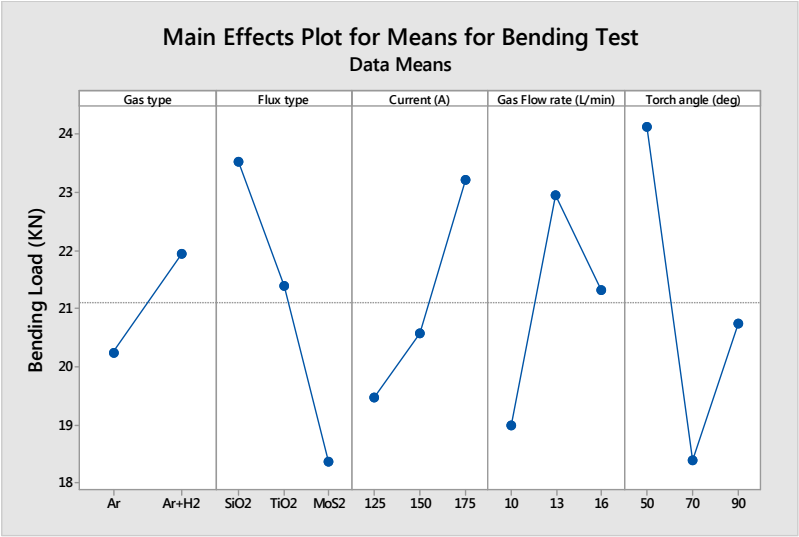

Figure 4.2: Plot for bending load of Duplex 2205

Figure 4.2 represents the main plot graph for the result. It represent that the bending samples having SiO_2 have more maximum bending load i.e. the SiO_2 flux causes more ductility , MoS_2 is found to be decreasing it. TiO_2 is found to be nominal in case of material Duplex 2205. Result shows that flux with SiO_2 affects the most the bending load i.e. SiO_2 increases the maximum bending load a material can bear before crack. It also represents that welding when done with 50º torch angle results in more ductility in comparison of 70º, 90º torch angle influenced average. When gas type is compared Ar +H_2 found to be leading factor than pure Ar. Reason can be considers for this is H_2 increase the fluidity of the molten pool and helps in getting higher penetration. When current is compared 175 A lead the influence when applied with fluxes SiO_2 TiO_2 and MoS_2. Similarly in case of gas flow rates 16L/min reasons for the ductility, 10L/min

responded average and 13 L/min was found low efficient gas rate or the process. In case of torch angle torch 50 ºand 90º, response is almost similar but for 70º response is less efficient.

Table 4.7: Response for bending load of Duplex 2205

Level	Gas type	Flux type	Current(A)	Gas Flow rate (L/min)	Torch angle(°)
1	20.24	23.53	19.48	18.98	24.13
2	21.94	21.38	20.57	22.97	18.39
3		18.36	23.22	21.32	20.75
Delta	1.71	5.17	3.75	3.98	5.74
Rank	5	2	4	3	1

Response of resulting factors is mentioned in Table 4.7. It was found that torch angle had highest value for delta of 5.74 followed by flux type's delta value = 5.17, gas flow rate's delta value = 3.98, current's delta value = 3.75 and with the least value for gas types = 1.71 It means that torch angle influence the most among these parameters and gas type influence least.

Table 4.8: Bent samples of material Duplex 2205

Experiment No 1	Experiment No 2	Experiment No 3
		
Experiment No 4	Experiment No 5	Experiment No 6
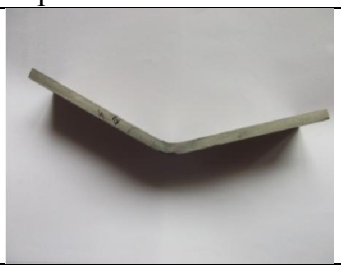		
Experiment No 7	Experiment No 8	Experiment No9
	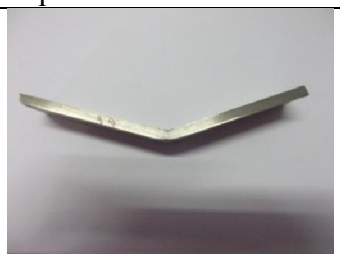	
Experiment No 10	Experiment No 11	Experiment No12
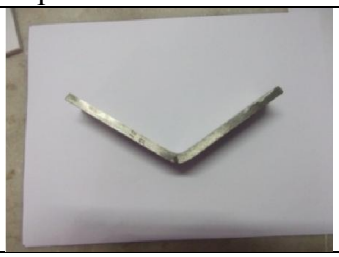		
Experiment No 13	Experiment No 14	Experiment No 15
		
Experiment No 16	Experiment No 17	Experiment No 18
		

4.3Toughness

Toughness is checked with the impact test. Here in this study charpy impact test is used.

4.3.1 Charpy impact test analysis for AISI 316

This is the result of Charpy Impact testing of all the samples in Table 4.9.

Table 4.9: Results of charpy impact test for two specimens of each AISI 316 weld samples.

Sl no.	Gas	Flux	Current (A)	Gas Flow rate (L/min)	Torch angle (°)	Toughness 1 (J)	Toughness 2 (J)	Toughness Avg (J)	SNR
1	Ar	SiO_2	125	10	50	80	59	69.5	36.54
2	Ar	SiO_2	150	13	70	88	74	81.0	38.07
3	Ar	SiO_2	175	16	90	54	66	60.0	35.43
4	Ar	TiO_2	125	10	70	66	102	84.0	37.88
5	Ar	TiO_2	150	13	90	66	86	76.0	37.39
6	Ar	TiO_2	175	16	50	82	86	84.0	38.47
7	Ar	MoS_2	125	13	50	62	62	62.0	35.84
8	Ar	MoS_2	150	16	70	60	52	56.0	34.89
9	Ar	MoS_2	175	10	90	56	106	81.0	36.90
10	Ar+H_2	SiO_2	125	16	90	51	88	69.5	35.90
11	Ar+H_2	SiO_2	150	10	50	86	90	88.0	38.89
12	Ar+H_2	SiO_2	175	13	70	48	54	51.0	34.10
13	Ar+H_2	TiO_2	125	13	90	64	52	58.0	35.12
14	Ar+H_2	TiO_2	150	16	50	72	78	75.0	37.48
15	Ar+H_2	TiO_2	175	10	70	106	88	97.0	39.62
16	Ar+H_2	MoS_2	125	16	70	33	34	33.5	30.49
17	Ar+H_2	MoS_2	150	10	90	52	36	44.0	32.43
18	Ar+H_2	MoS_2	175	13	50	54	44	49.0	33.68

There were two samples for Charpy Impact test for each experiment. In Table 4.9 average of the result for each sample is calculated also signal to noise ratio is also listed for each sample.

According to result sample 15 has highest average toughness = 97.0 J which has varying parameters gas= Ar+H_2, flux = TiO_2, current =175 A, gas flow rate = 10 L/min, and torch angle 70°. Sample 16 has the lowest average toughness =33.5 J which has varying parameters gas= Ar+H_2, flux = MoS_2, current =125 A, gas flow rate = 16 L/min, and torch angle 70°.

When applied ANOVA on these results it was found that these factors influencing in a decreasing order of flux , gas flow rate, current, gas type and torch angle according to Table 4.10.

Table 4.10: ANOVA for toughness for AISI 316

Source	DF	SS (Seq)	SS (Adj)	MS (Adj)	F value	P value
Gas	1	435.1	435.1	435.12	2.35	0.164
Flux	2	1878.9	1878.9	939.43	5.08	0.038
Current (A)	2	220.4	220.4	110.18	0.60	0.574
Gas Flow rate (L/min)	2	821.9	821.9	410.93	2.22	0.171
Torch angle(°)	2	130.1	130.1	65.06	0.35	0.714
Residual error	8	1480.8	1480.8	185.09		
Total	17	4967.1				

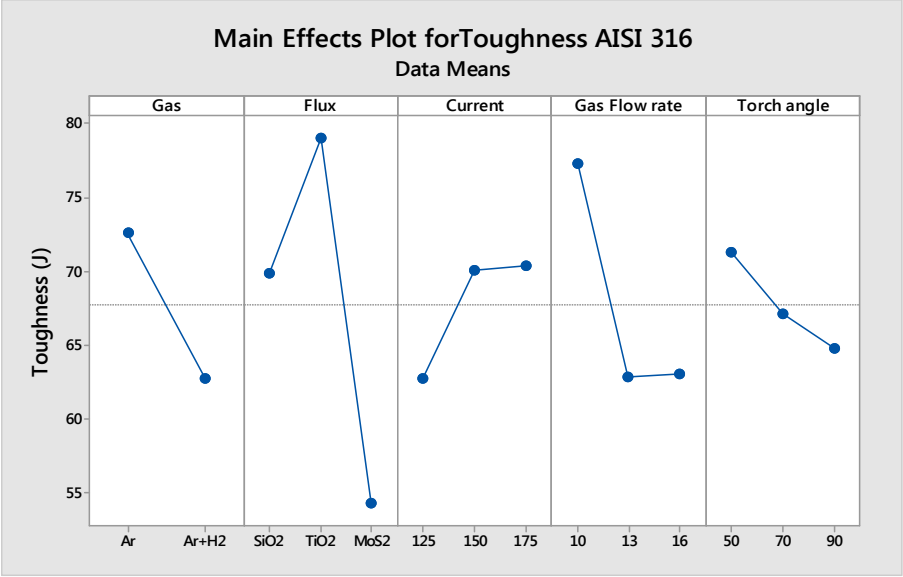

Figure 4.3: Main plot graph for toughness for AISI 316

It was found that samples get better toughness due to shielding gas Ar, H_2 might have blown with the pores. In case of flux type TiO_2 impact is positive than SiO_2 and MoS_2 and 175 A current is favorable if current is considered than 150 A and 125A.

Gas flow rate = 10 L/min supports the toughness more than 13 L/min and 16 L/min. Torch angle 50º is found most suitable to achieve the higher toughness as it is in the main plot graph than 70º and 90º.

According to response table flux has maximum delta value indicated the maximum influence of this parameter on the process, it has followed by gas flow rate with delta values 14.42 and, other factors were also found to be significant in an order; gas type, current and the torch angle came.

Table 4.11: Response for toughness for AISI 316

Level	Gas	Flux	Current(A)	Gas Flow rate(L/min)	Torch angle(°)
1	72.61	69.83	62.75	77.25	71.25
2	62.78	79.00	70.00	62.83	67.08
3		54.25	70.33	63.00	64.75
Delta	9.83	24.75	7.58	14.42	6.50
Rank	3	1	4	2	5

Table 4.12: ANOVA for SN ratios for toughness for AISI 316

Source	DF	SS (Seq)	SS (Adj)	MS (Adj)	F value	P value
Gas	1	10.456	10.456	10.456	3.50	0.098
Flux	2	40.976	40.976	20.488	6.85	0.018
Current (A)	2	5.340	5.340	2.670	0.89	0.447
Gas Flow rate(L/min)	2	8.834	8.834	4.417	1.48	0.285
Torch angle(°)	2	5.374	5.374	2.687	0.90	0.445
Residual error	8	23.925	23.925	2.991		
Total	17	94.905				

Results from SN ratios table validates the result mentioned earlier similarly the plot validate the plot by main effect.

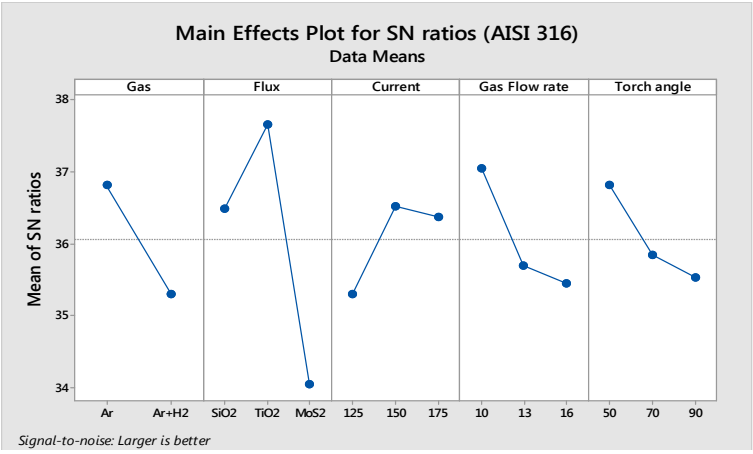

Figure 4.4: SN ratio plot for toughness of AISI 316

Signal to noise ratio is analysed for larger the better option. And it absolutely supports the main plot.

4.3.2 Charpy impact test analysis for Duplex 2205

The result is been discussed in Table 4.13 There were two samples for Charpy Impact test for each experiment. According to result sample 12 has highest average toughness = 85.0 J and sample 8 has the lowest average toughness = 32.5 J.

Experiment no. 12 has the parameters flux type SiO_2 current =175A gas flow rate = 13 L/min and torch angle = 70º. Experiment no 8 has gas type Ar flux type = MoS_2, current 150 A, gas flow rate =16 L/min and torch angle =70º.

Table 4.13: Results of charpy impact test for two specimens of each Duplex 2205 weld samples.

Sl. No.	Gas Type	Flux Type	Current (A)	Gas Flow rate (L/min)	Torch angle (°)	Toughness 1 (J)	Toughness 2 (J)	Average Toughness (J)	SNR
1	Ar	SiO_2	125	10	50	58	58	58.0	35.26
2	Ar	SiO_2	150	13	70	58	38	48.0	33.05
3	Ar	SiO_2	175	16	90	72	83	77.5	37.72
4	Ar	TiO_2	125	10	70	44	53	48.5	33.60
5	Ar	TiO_2	150	13	90	75	55	65.0	35.94
6	Ar	TiO_2	175	16	50	64	100	82.0	37.64
7	Ar	MoS_2	125	13	50	50	61	55.5	34.75
8	Ar	MoS_2	150	16	70	31	34	32.5	30.20
9	Ar	MoS_2	175	10	90	51	48	49.5	33.88
10	Ar+H_2	SiO_2	125	16	90	66	65	65.5	36.32
11	Ar+H_2	SiO_2	150	10	50	60	90	75.0	36.97
12	Ar+H_2	SiO_2	175	13	70	95	75	85.0	38.40
13	Ar+H_2	TiO_2	125	13	90	102	48	75.0	35.76
14	Ar+H_2	TiO_2	150	16	50	87	76	81.5	38.16
15	Ar+H_2	TiO_2	175	10	70	54	63	58.5	35.26
16	Ar+H_2	MoS_2	125	16	70	51	40	45.5	32.96
17	Ar+H_2	MoS_2	150	10	90	36	52	44.0	32.43
18	Ar+H_2	MoS_2	175	13	50	50	48	49.0	33.79

Analysis of variance for these results is mentioned in Table 4.14. It was found that flux influenced most the result and other factors were also found to be influencing in a sequence of torch angle, current, gas flow rate and least affected by gas type.

Table 4.14: ANOVA for toughness of Duplex 2205 welds samples.

Source	DF	SS (Seq)	SS (Adj)	MS (Adj)	F value	P value
Gas	1	217.0	217.0	217.01	2.38	0.162
Flux	2	1987.9	1987.9	993.93	10.90	0.005
Current (A)	2	330.4	330.4	165.18	1.81	0.225
Gas Flow rate(L/min)	2	254.8	254.8	S127.39	1.40	0.302
Torch angle(°)	2	606.2	606.2	303.10	3.32	0.089
Residual Error	8	729.7	729.7	91.21		
Total	17	4125.9				

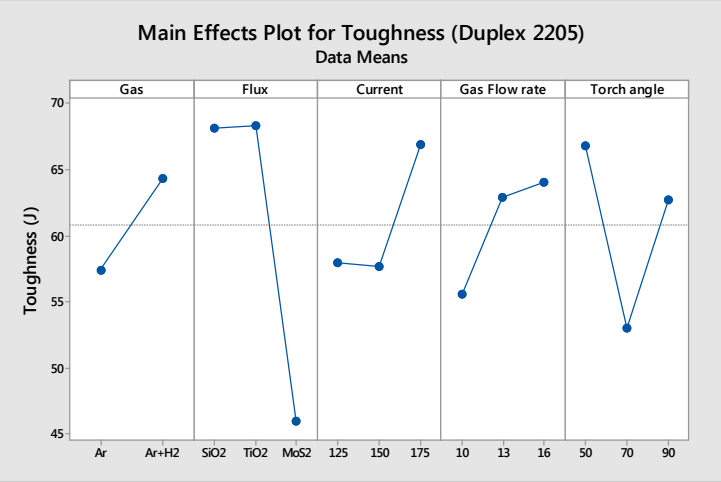

Figure 4.5: Plot for toughness of Duplex 2205

The graph plot in the Fig. 4.5 represents that shielding gas type Ar + H_2 is more significant than the shielding gas Ar in case of Duplex 2205 weld samples. Reason can be considers for this is H_2 increase the fluidity of the molten pool and helps in getting higher penetration. TiO_2 is also a preferable flux factor along wither highest significant level. SiO_2 performed almost similar and MoS_2 is found to be diminishing effect. When different currents were compared 175 A stood most significant than the different currents 125A and 150 A in a sequence. Gas flow rate is found optimal at 16 L/min than 13/L/min and 10L/min. i.e. larger the gas flow rate larger the influence In case of torch angle 50º has the more significant result than 90º and 70°.

Table 4.15 represents the response values with delta values of each factor and their rank. It is found that flux is the most significant factor with delta value 22.42 and gas type is the least significant factor with delta value 6.94.

Table 4.15: Response for toughness of Duplex 2205

Level	Gas	Flux	Current(A)	Gas Flow rate(L/min)	Torch angle(°)
1	57.39	68.17	58.00	55.58	66.83
2	64.33	68.42	57.67	62.92	53.00
3		46.00	66.92	64.08	62.75
Delta	6.94	22.42	9.25	8.50	13.83
Rank	5	1	3	4	2

Table 4.16: ANOVA for SN ratios for toughness of Duplex 2205

Source	DF	SS (Seq)	SS (Adj)	MS (Adj)	F value	P value
Gas	1	3.575	3.575	3.575	1.99	0.196
Flux	2	40.348	40.348	20.174	11.23	0.005
Current (A)	2	9.254	9.254	4.627	2.58	0.137
Gas Flow rate(L/min)	2	2.866	2.866	1.433	0.80	0.483
Torch angle(°)	2	14.747	14.747	7.374	4.10	0.059
Residual Error	8	14.375	14.375	1.797		
Total	17	85.165				

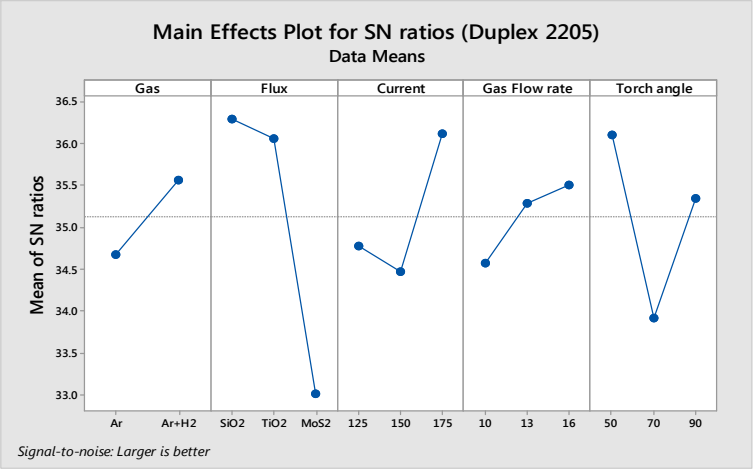

Figure 4.6: SN ratio plots for toughness of Duplex 2205

Table 4.16 and Fig. 4.6 represent ANOVA and plot for SN ratios for duplex 2205 weld samples. It was found that all the factors are similarly contributing as earlier ANOVA table. Analysis of signal to noise ratio validates the results.

4.4 Microhardness variation

After etching by the etchant Carpenter samples were indented in the Microhardness tester. The whole key behind indent is larger the indent smaller the microhardness and smaller the indent larger the hardness. It is calculated with the dimensions of the indent found on the specimen.

4.4.1 Microhardness variation for AISI 316 welds

Table 4.17: Orthogonal array with microhardness at fusion zone AISI 316 weld

Sl no.	Gas	Flux	Current (A)	Gas Flow rate (L/min)	Torch angle (°)	HVN 1	HVN 2	HVN 3	Average HVN	SNR
1	Ar	SiO_2	125	10	50	384.34	372.67	392.78	383.26	51.66
2	Ar	SiO_2	150	13	70	322.56	335.80	304.68	321.01	50.10
3	Ar	SiO_2	175	16	90	389.25	406.54	399.96	398.58	52.00
4	Ar	TiO_2	125	10	70	408.90	405.99	404.39	406.43	52.17
5	Ar	TiO_2	150	13	90	428.86	438.34	410.52	425.90	52.57
6	Ar	TiO_2	175	16	50	418.14	422.80	404.60	415.18	52.36
7	Ar	MoS_2	125	13	50	233.98	230.07	240.05	234.70	47.40
8	Ar	MoS_2	150	16	70	422.99	422.88	422.88	422.91	52.52
9	Ar	MoS_2	175	10	90	364.99	366.54	378.59	370.04	51.36
10	Ar+H_2	SiO_2	125	16	90	322.56	344.83	334.14	333.84	50.46
11	Ar+H_2	SiO_2	150	10	50	238.25	244.71	242.47	241.81	47.66
12	Ar+H_2	SiO_2	175	13	70	333.65	323.66	320.44	325.92	50.25
13	Ar+H_2	TiO_2	125	13	90	237.73	232.01	238.00	235.91	47.45
14	Ar+H_2	TiO_2	150	16	50	313.15	322.56	332.41	322.71	50.16
15	Ar+H_2	TiO_2	175	10	70	276.75	275.33	271.72	274.60	48.77
16	Ar+H_2	MoS_2	125	16	70	480.78	492.57	442.66	472.00	53.45
17	Ar+H_2	MoS_2	150	10	90	262.81	253.47	266.41	260.89	48.32
18	Ar+H_2	MoS_2	175	13	50	438.14	458.42	447.83	448.13	53.02

The initial result suggest the average highest microhardness was achieved by experiment no 18 which is weld with parameters shielding gas type = Ar+H_2, flux type = MoS_2, current =175 A, gas flow rate 13 L/min and torch angle = 50°.

The lowest microhardness achieved by experiment no experiment no 7 which was weld with parameters gas type = Ar, flux type = MoS_2, current =125 A, gas flow rate 13 L/min and torch angle = 50°.

Table 4.18: ANOVA for microhardness at fusion zone of AISI 316 weld

Source	DF	SS (Seq)	SS (Adj)	MS (Adj)	F value	P value
Gas	1	11869	11869	11869	1.62	0.239
Flux	2	3551	3551	1775	0.24	0.790
Current (A)	2	4942	4942	2471	0.34	0.723
Gas Flow rate (L/min)	2	18108	18108	9054	1.24	0.340
Torch angle(°)	2	3937	3937	1969	0.27	0.771
Residual Error	8	58551	58551	7319		
Total	17	100958				

According to ANOVA Table 4.17 contribution made by different parameters plays the major role contribution made by gas flow rate is higher in case of fusion zone of the weld sample of material AISI 316. Followed by parameters gas types, current, torch angle and flux.

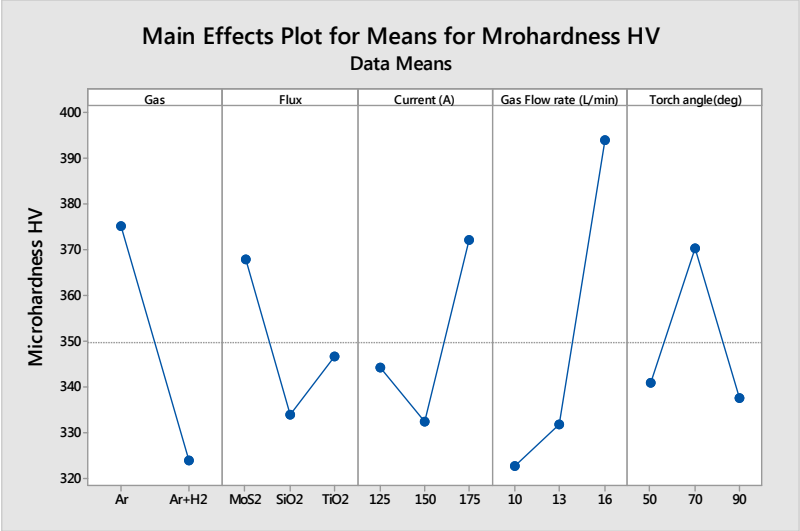

Figure 4.7: Plot for microhardness at Fusion zone of AISI 316 welds

Main graph plot implies that pure Ar leads to more microhardness at its fusion zone than the Ar+H_2. In case of flux MoS_2 lead the responsibility of occurring microhardness and followed by TiO_2 and SiO_2. When current were compared 175 A caused maximum hardness followed by two different currents 125 A and 150 A; gas flow rate 16 L/min caused great impact on the microhardness. When torch angles were compared 70º enriched the microhardness than 50º and 90°.

Table 4.19: Response for means microhardness at fusion zone of AISI 316 weld

Level	Gas	Flux	Current(A)	Gas Flow rate(L/min)	Torch angle(°)
1	375.3	368.1	344.4	322.8	341.0
2	324.0	334.1	332.5	331.9	370.5
3		346.8	372.1	394.2	337.5
Delta	51.4	34.0	39.5	71.4	32.9
Rank	2	4	3	1	5

Response table supports the same gas flow rate has highest delta value and torch angle least affected it by delta value mean while gas type, current and flux also had impact on microhardness in a decreasing contribution order.

Table 4.20: ANOVA for SN ratios for the fusion zone of AISI 316

Source	DF	SS (Seq)	SS (Adj)	MS (Adj)	F value	P value
Gas	1	55.09	55.09	55.09	0.29	0.60
Flux	2	123.64	123.64	61.82	0.32	0.73
Current (A)	2	111.04	111.04	55.52	0.29	0.75
Gas Flow rate (L/min)	2	80.88	80.88	40.44	0.21	0.81
Torch angle(°)	2	226.39	226.39	113.20	0.59	0.57
Residual Error	8	1544.04	1544.04	193.00		
Total	17	2141.08				

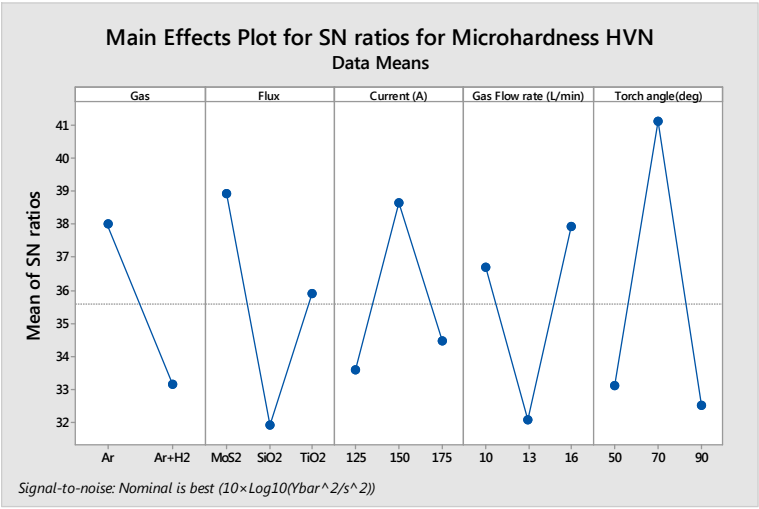

Figure 4.8: Plot for SN ratio for microhardness at Fusion zone of AISI 316 welds

Table 4.21: Response for means SN ratios for microhardness at fusion zone of AISI 316

Level	Gas	Flux	Current(A)	Gas Flow rate (L/min)	Torch angle(°)
1	38.03	38.94	33.59	36.70	33.10
2	33.13	31.90	38.67	32.08	41.15
3		35.88	34.48	37.95	32.49
Delta	4.90	7.04	5.08	5.87	8.66
Rank	5	2	4	3	1

Response table suggest that torch angle has much influence on the microstructure. As its delta value is highest among all 8.66 after that flux has delta value 7.04, gas flow rate has delta value 5.87, current has delta value 5.08 and gas type has lowest 4.90. Delta values decide the rank of all the parameters used in this study.

Table 4.22: Orthogonal array with microhardness at HAZ of AISI 316 weld

Sl no.	Gas	Flux	Current (A)	Gas Flow rate (L/min)	Torch angle (°)	HVN 1	HVN 2	HVN 3	Average HVN	SNR
1	Ar	SiO_2	125	10	50	380.77	377.23	364.86	374.29	51.45
2	Ar	SiO_2	150	13	70	364.83	349.86	368.72	361.13	51.14
3	Ar	SiO_2	175	16	90	346.99	365.30	357.80	356.69	51.04
4	Ar	TiO_2	125	10	70	399.96	387.98	391.31	393.08	51.88
5	Ar	TiO_2	150	13	90	362.65	382.74	378.59	374.66	51.46
6	Ar	TiO_2	175	16	50	399.96	374.84	382.94	385.91	51.72
7	Ar	MoS_2	125	13	50	246.25	243.84	259.38	249.82	47.94
8	Ar	MoS_2	150	16	70	395.60	378.86	387.09	387.18	51.75
9	Ar	MoS_2	175	10	90	386.95	380.56	374.51	380.67	51.60
10	Ar+H_2	SiO_2	125	16	90	287.24	269.25	279.70	278.73	48.89
11	Ar+H_2	SiO_2	150	10	50	384.92	368.72	373.03	375.55	51.48
12	Ar+H_2	SiO_2	175	13	70	326.94	340.56	344.10	337.20	50.55
13	Ar+H_2	TiO_2	125	13	90	246.36	244.56	244.22	245.04	47.78
14	Ar+H_2	TiO_2	150	16	50	368.72	339.23	349.86	352.60	50.93
15	Ar+H_2	TiO_2	175	10	70	244.22	276.75	281.92	267.63	48.49
16	Ar+H_2	MoS_2	125	16	70	442.66	437.58	453.07	444.44	52.95
17	Ar+H_2	MoS_2	150	10	90	297.57	286.60	292.01	292.06	49.30
18	Ar+H_2	MoS_2	175	13	50	418.00	399.92	413.48	410.46	52.26

According to Table 4.22 highest Average Microhardness found in experiment no 16 where gas parameters shielding gas type = Ar+H_2, flux type = MoS_2, current =125 A, gas flow rate 16 L/min and torch angle = 70°.

The lowest microhardness achieved by experiment no experiment no 17 which was weld with parameters gas type = Ar+H_2, flux type = MoS_2, current =150 A, gas flow rate 10 L/min and torch angle = 90°.

Table 4.23: ANOVA for microhardness at HAZ of AISI 316

Source	DF	SS (Seq)	SS (Adj)	MS (Adj)	F value	P value
Gas	1	3748	3748	3747.7	0.80	0.396
Flux	2	1777	1777	888.4	0.19	0.830
Current (A)	2	2688	2688	1343.9	0.29	0.757
Gas Flow rate (L/min)	2	4311	4311	2155.6	0.46	0.646
Torch angle(°)	2	6644	6644	3321.8	0.71	0.519
Residual Error	8	37281	37281	4660.1		
Total	17	56448				

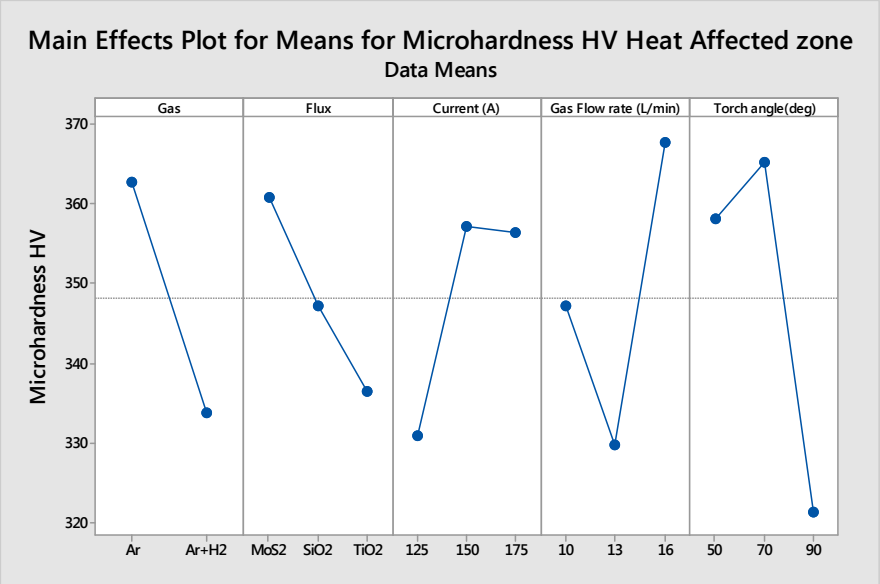

Figure 4.9: Plot for microhardness at HAZ

ANOVA Table 4.23 suggest that the torch angle is contributing the highest for the result the sequence for contributing factor is torch angle, gas flow rate, gas type, current and least

contributing is flux. The reason behind it can be flux made material ductile on the welds so it is in last in contributing index.

Table 4.24: Response for microhardness at HAZ of AISI 316 welds

Level	Current(A)	Gas	Flux	Gas Flow rate (L/min)	Torch angle (°)
1	330.9	362.6	360.8	347.2	358.1
2	357.2	333.7	347.3	329.7	365.1
3		356.4	336.5	367.6	321.3
Delta	26.3	28.9	24.3	37.9	43.8
Rank	4	3	5	2	1

Table 4.25: ANOVA for SN ratios microhardness at HAZ of AISI 316

Source	DF	SS (Seq)	SS (Adj)	MS (Adj)	F value	P value
Gas	4.607	1	4.607	4.607	0.18	0.680
Flux	3.711	2	7.423	7.423	0.15	0.865
Current (A)	45.042	2	90.084	90.084	1.79	0.228
Gas Flow rate (L/min)	19.606	2	39.213	39.213	0.78	0.491
Torch angle(°)	44.587	2	89.174	89.174	1.77	0.231
Residual Error	25.204	8	201.633	201.633		
Total		17	432.134			

When ANOVA of signal to noise is calculated it was found contribution of current was most in the microhardness when analyzed for nominal is better. Too hard material is not good also. Analysis suggests current and the torch angle were most affecting parameters. Followed by gas flow rate, flux and gas type in an order.

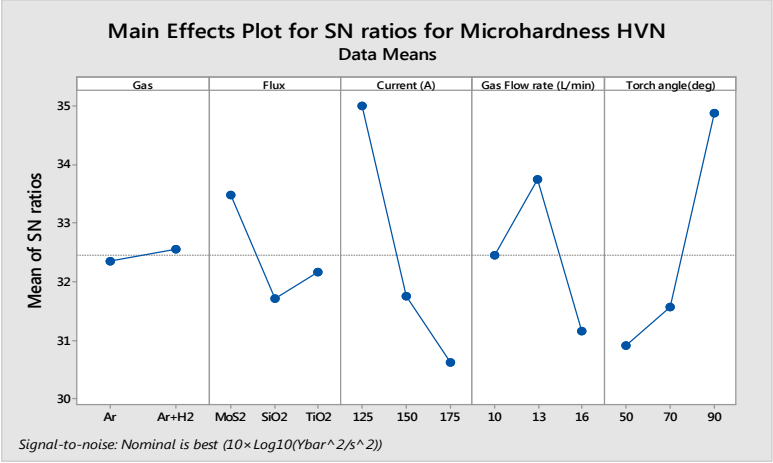

Figure 4.10: SN ratio plot for microhardness at HAZ

Plot also validates the result. It suggests Ar +H_2 as leading than Ar. When compared different current levels 125A had the best result than 150 A and 175A, among flux MoS_2 lead the result followed by TiO_2 and SiO_2, when gas flow rates were compared. 13L/min lead and followed by 10L/min and 16L/min respectively, among torch angles 90º stood best for this result when compared with 70 º and 50°.

Table 4.26: Response table microhardness at HAZ of AISI 316 weld

Level	Gas	Flux	Current(A)	Gas Flow rate(L/min)	Torch angle(°)
1	32.3	33.48	34.99	32.45	30.90
2	5	31.70	31.74	33.74	31.56
3	32.5	32.16	30.60	31.15	34.89
Dela	50.20	1.78	4.39	2.59	3.99
Rank	5	4	1	3	2

Response table suggest current was the most influencing parameter as higher current lead to high depth of penetration .torch angle is following the result after current levels. It further followed by gas flow rate flux and gas type respectively.

4.4.2 Microhardness variation for duplex 2205 welds

There are possibilities to achieve larger variation even on a single specimen; so, three indents were made on each zone of the specimen i.e. three in fusion zone and three in HAZ

Table 4.27: Orthogonal array with microhardness at fusion zone of duplex 2205 weld

Sl no.	Gas type	Flux type	Current (A)	Gas Flow rate (L/min)	Torch angle (°)	HVN (1)	HVN (2)	HVN (3)	Average HVN	SNR
1	Ar	SiO_2	125	10	50	507.45	565.95	524.04	532.48	54.49
2	Ar	SiO_2	150	13	70	322.56	335.86	304.68	321.03	50.11
3	Ar	SiO_2	175	16	90	329.08	349.86	329.08	336.00	50.51
4	Ar	TiO_2	125	10	70	369.76	348.41	352.73	356.96	51.04
5	Ar	TiO_2	150	13	90	334.54	318.14	324.68	325.78	50.25
6	Ar	TiO_2	175	16	50	444.79	465.96	477.12	462.62	53.29
7	Ar	MoS_2	125	13	50	511.10	524.04	537.48	524.20	54.38
8	Ar	MoS_2	150	16	70	488.40	433.26	459.59	460.41	53.23
9	Ar	MoS_2	175	10	90	374.84	391.31	382.94	383.03	51.66
10	Ar+H_2	SiO_2	125	16	90	322.56	334.83	314.00	323.79	50.19
11	Ar+H_2	SiO_2	150	10	50	325.80	346.26	342.72	338.26	50.57
12	Ar+H_2	SiO_2	175	13	70	400.03	428.26	404.54	410.94	52.26
13	Ar+H_2	TiO_2	125	13	90	340.56	326.94	317.25	328.25	50.31
14	Ar+H_2	TiO_2	150	16	50	418.57	470.80	293.43	394.26	51.38
15	Ar+H_2	TiO_2	175	10	70	532.44	519.30	519.83	523.85	54.38
16	Ar+H_2	MoS_2	125	16	70	408.90	399.96	387.09	398.65	52.00
17	Ar+H_2	MoS_2	150	10	90	395.60	382.94	374.84	384.46	51.69
18	Ar+H_2	MoS_2	175	13	50	447.82	458.42	453.07	453.10	53.12

Table 4.28: ANOVA for microhardness at fusion zone of duplex 2205

Source	DF	SS (Seq)	SS (Adj)	MS (Adj)	F value	P value
Gas	1	1200	1200	1200	0.28	0.612
Flux	2	9901	9901	4950	1.15	0.365
Current (A)	2	10444	10444	5222	1.21	0.347
Gas Flow rate(L/min)	2	2497	2497	1248	0.29	0.756
Torch angle(°)	2	33096	33096	16548	3.83	0.068
Residual Error	8	34526	34526	4316		
Total	17	91664				

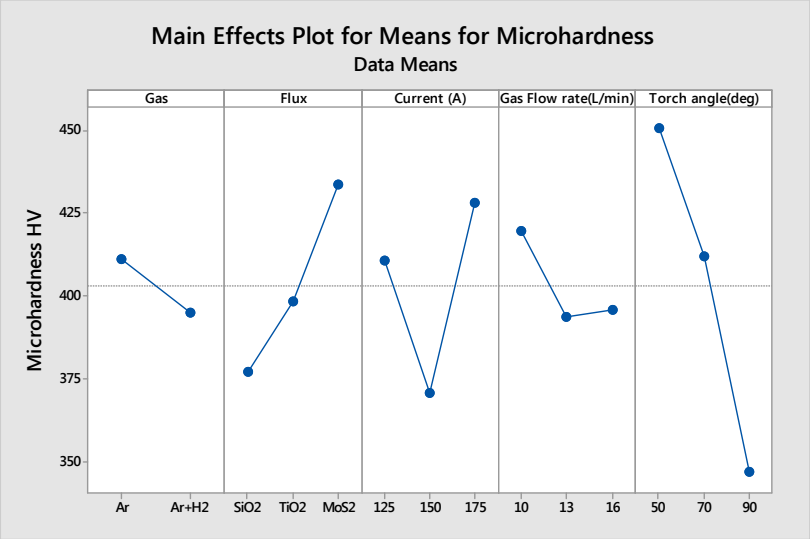

Figure 4.11: Microhardness Plot for fusion zone of Duplex 2205 welds

Table 4.29: Response for microhardness at fusion zone of duplex 2205 weld

Level	Gas	Flux	Current(A)	Gas Flow rate (L/min)	Torch angle (°)
1	411.4	377.1	410.7	419.8	450.8
2	395.1	398.6	370.7	393.9	412.0
3		434.0	428.3	396.0	346.9
Delta	16.3	56.9	57.6	26.0	103.9
Rank	5	3	2	4	1

Table 4.29 implies that torch angle affects the most the microhardness at the fusion zone of the Duplex 2205 welds. Current, flux and gas flow rate also add contribution towards it in respective order but gas type affects the least.

Table 4.30: ANOVA for SN ratios for microhardness at fusion zone of duplex 2205

Source	DF	SS (Seq)	SS (Adj)	MS (Adj)	F value	P value
Gas	1	5.367	5.367	5.367	0.19	0.677
Flux	2	27.176	27.176	13.588	0.47	0.639
Current (A)	2	83.507	83.507	41.753	1.45	0.289
Gas Flow rate(L/min)	2	96.184	96.184	48.092	1.67	0.247
Torch angle(°)	2	76.845	76.845	38.422	1.34	0.315
Residual Error	8	229.714	229.714	28.714		
Total	17	518.792				

Table 4.30 suggests signal to noise ratio for the result found in ANOVA table earlier. It explains that gas flow rate among all the parameters affects the microhardness most followed by current, torch angle, flux and gas type.

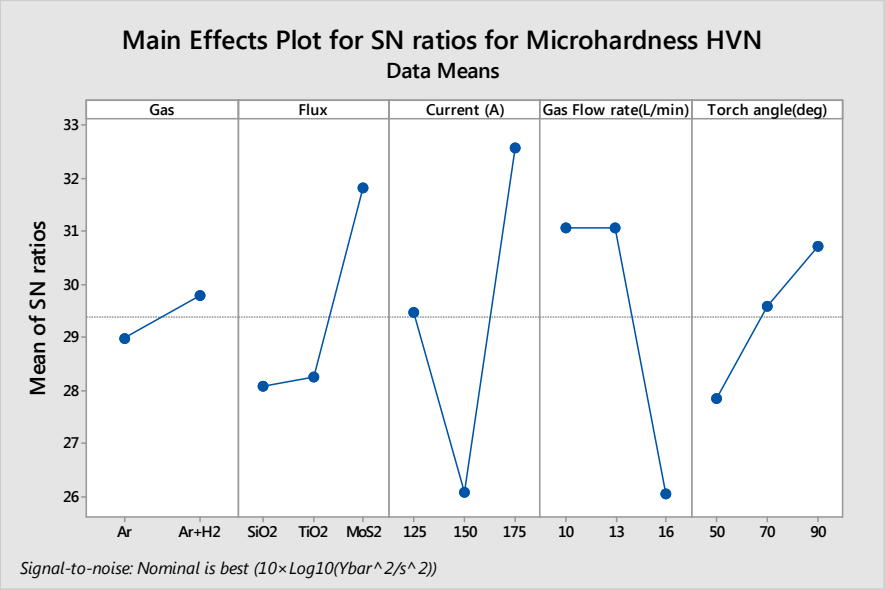

Figure 4.12: SN plot for microhardness at fusion zone of Duplex 2205 welds

The signal to noise plot suggest shielding gas Ar+H_2 increased the microhardness at the fusion zone of duplex 2205 weld joint than pure Ar. Flux MoS_2 also created great affect in increasing the microhardness than TiO_2 and SiO_2 in an order. Higher current 175A increased the microhardness followed by current levels 125 A and 150 A in an order. Gas flow rate of 10 L/min and 13L/min increased the microhardness .higher torch angle 90º increased the microhardness followed by 70º and 50º in an order.

Table 4.31: Response for means SN ratios for microhardness at fusion zone of duplex 2205

Level	Gas	Flux	Current (A)	Gas Flow rate (L/min)	Torch Angle (°)
1	28.98	28.07	29.48	31.06	27.85
2	29.79	28.26	26.08	31.07	29.59
3		31.82	32.59	26.02	30.71
Delta	0.80	3.76	6.51	5.05	2.87
Rank	5	3	1	2	4

Nominal is best (10× Log 10(Ybar^2/s^2))

Table 4.32: Orthogonal array with microhardness at HAZ of Duplex 2205 weld

Sl no.	Gas	Flux	Current (A)	Gas Flow rate (L/min)	Torch angle (°)	HVN 1	HVN 2	HVN 3	Average HVN	SNR
1	Ar	SiO_2	125	10	50	544.39	558.62	544.39	549.13	54.79
2	Ar	SiO_2	150	13	70	364.83	349.86	368.72	361.13	51.14
3	Ar	SiO_2	175	16	90	364.26	349.86	361.00	358.37	51.08
4	Ar	TiO_2	125	10	70	480.78	463.86	480.78	475.14	53.53
5	Ar	TiO_2	150	13	90	324.68	475.04	382.94	394.22	51.60
6	Ar	TiO_2	175	16	50	439.72	444.79	471.49	452.00	53.09
7	Ar	MoS_2	125	13	50	463.86	408.90	486.62	453.12	53.05
8	Ar	MoS_2	150	16	70	369.27	346.99	376.99	364.41	51.21
9	Ar	MoS_2	175	10	90	327.92	327.92	348.97	334.93	50.48
10	Ar+H_2	SiO_2	125	16	90	259.72	287.24	269.25	272.07	48.67
11	Ar+H_2	SiO_2	150	10	50	326.26	298.34	304.14	309.58	49.79
12	Ar+H_2	SiO_2	175	13	70	438.34	465.14	454.13	452.54	53.10
13	Ar+H_2	TiO_2	125	13	90	391.31	351.35	347.70	363.45	51.17
14	Ar+H_2	TiO_2	150	16	50	326.94	320.44	329.13	325.50	50.24
15	Ar+H_2	TiO_2	175	10	70	450.93	535.50	515.49	500.64	53.91
16	Ar+H_2	MoS_2	125	16	70	374.82	370.88	399.96	381.88	51.62
17	Ar+H_2	MoS_2	150	10	90	395.60	355.67	374.84	375.37	51.46
18	Ar+H_2	MoS_2	175	13	50	437.58	458.43	422.88	439.63	52.84

Table 4.33: ANOVA for means of microhardness at HAZ of Duplex 2205 welds

Source	DF	SS (Seq)	SS (Adj)	MS (Adj)	F value	P value
Gas	1	5753	5753	5753	1.68	0.231
Flux	2	3977	3977	1989	0.58	0.581
Current (A)	2	16732	16732	8366	2.44	0.148
Gas Flow rate(L/min)	2	14169	14169	7085	2.07	0.189
Torch angle(°)	2	20927	20927	10463	3.06	0.103
Residual Error	8	27376	27376	3422		
Total	17	88935				

Contribution of parameter torch angle was found to be most influencing followed by current gas flow rate, gas type and flux in an order.

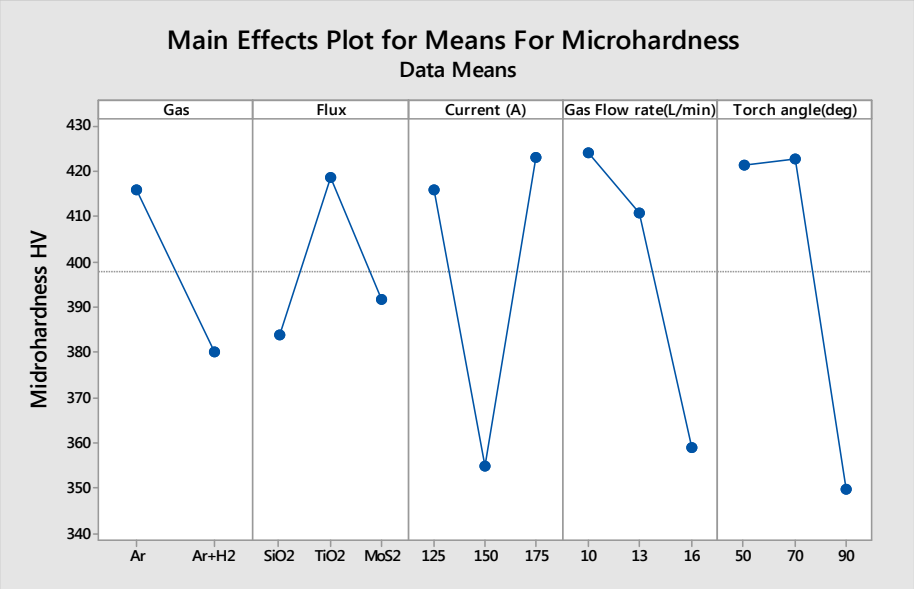

Figure 4.13: Plot for microhardness at HAZ

It suggest pure Ar helped weld to achieve better microhardness than Ar+H_2. TiO_2 flux lead the influence contribution and that is followed by SiO_2 and TiO_2. Current 175 Affected most the microstructure when compared with 125 A and 150 A. In case gas flow rate 10 L/min leads the result than 13 L/min and 16L/m. In case of torch angle 70º were found most contributing parameter when compared with other gas flow rates 50º and 90º in a diminishing sequence

Table 4.34: Response for microhardness at HAZ (duplex 2205)

Level	Gas	Flux	Current(A)	Gas Flow rate(L/min)	Torch angle(°)
1	415.8	383.8	415.8	424.1	421.5
2	380.1	418.5	355.0	410.7	422.6
3		391.6	423.0	359.0	349.7
Delta	35.8	34.7	68.0	65.1	72.9
Rank	4	5	2	3	1

Response found for HAZ is same as the fusion zone torch angle influence the microhardness most Followed by Current, gas flow rate, gas type and flux type.

Table 4.35: ANOVA for SN ratios for microhardness at HAZ (Duplex 2205)

Source	DF	SS (Seq)	SS (Adj)	MS (Adj)	F value	P value
Gas	1	0.252	0.252	0.2517	0.01	0.940
Flux	2	97.362	97.362	48.6812	1.17	0.360
Current (A)	2	0.054	0.054	0.0268	0.00	0.999
Gas Flow rate(L/min)	2	127.135	127.135	63.5676	1.52	0.275
Torch angle(°)	2	24.366	24.366	12.1832	0.29	0.755
Residual Error	8	334.121	334.121	41.7651		
Total	17	583.290				

According to ANOVA table contribution of gas flow rate is most among all the factors. Flux is also influencing the result followed by influencing effects torch angle, gas type, and current.

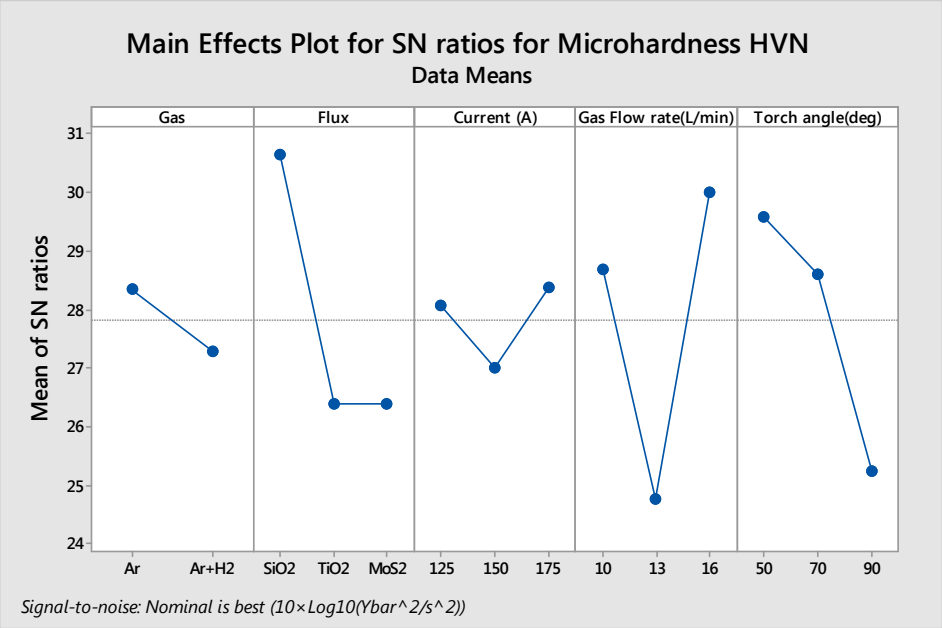

Figure 4.14: SN ratio plot for microhardness at HAZ

Plot for SN ratio result shows pure argon has better effect on microhardness. As shielding Ar+H_2 makes material more ductile after that it suggest SiO_2 gives the better result than TiO_2 and MoS_2 in case of material Duplex 2205. 150 A current has lowest influence on microhardness and 175 A and 125 A are found nominal effecting parameter. Gas flow rate 10 L/min is nominal and its effect on microhardness is dominated by the 16 L/min, 13 L/min could not make much difference in microhardness. In case of torch angle 50º reached the peak followed by angles 70º and 90º in an order.

Table 4.36: Response for means SN ratios for microhardness at HAZ

Level	Gas	Flux	Current (A)	Gas Flow rate(L/min)	Torch angle (°)
1	28.33	30.66	28.06	28.68	29.58
2	27.28	26.38	27.00	24.75	28.60
3		26.38	28.37	30.00	25.24
Delta	1.06	4.29	1.37	5.25	4.34
Rank	5	3	4	1	2

Response for signal to noise ration suggest that gas flow rate is the most influencing parameter among all. Then torch angle has is effect on result followed by flux, current, and gas type.

4.5 Metallurgical Observation

Each sample has been observed through metallurgical Microscope through different lenses 100X, 200X and 500X for better vision of their structure in their fusion zone and heat affected zone. All the images taken are there with their experimental parameters.

4.5.2 Metallurgical Observation for AISI 316

For austenitic steel AISI 316 samples were etched with Carpenter etchant. After welding molten pool gets solidified from the liquid form to ferrite phase as the pool austenitic portion is visible in most of the portion with some larger black veins of ferrite after etching. Different sized veins were found in different experiments as shown in the Table 4.37.

Table 4.37 : Microstructure of all the experiment of the AISI 316

100X	200X	500X
Experiment No. 1 Shielding Gas type = Ar, Flux used = SiO_2, Current = 125 A, Gas flow Rate = 10 L /min, Torch angle = 50°.		
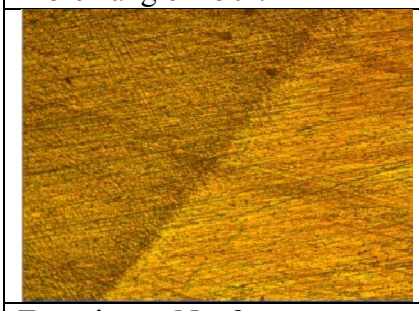	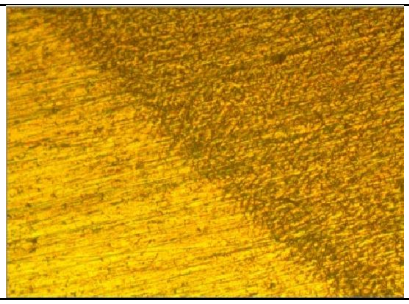	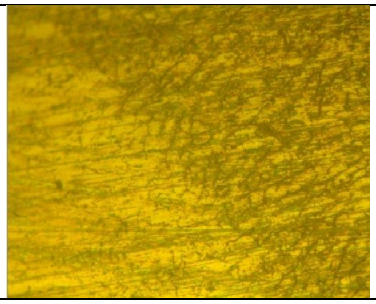
Experiment No. 2 Shielding Gas type = Ar, Flux used = SiO_2, Current = 150 A, Gas flow Rate = 13 L/min, Torch angle = 70°.		
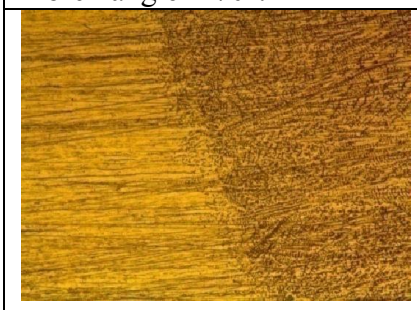	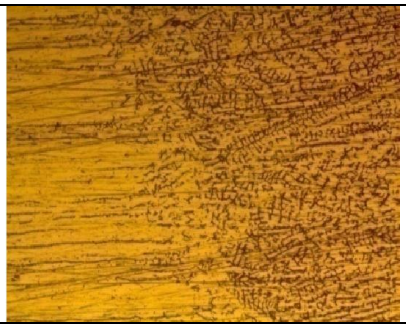	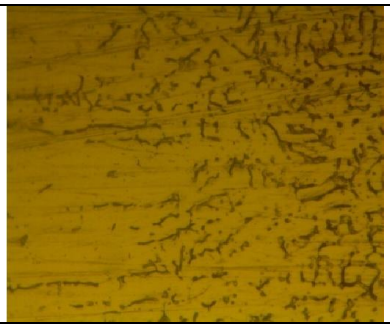
Experiment No. 3 Shielding Gas type = Ar, Flux used = SiO_2, Current = 175 A, Gas flow Rate = 16 L /min, Torch angle = 90°.		
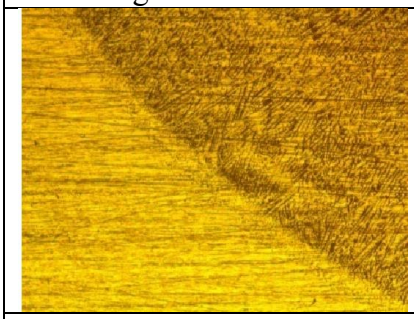		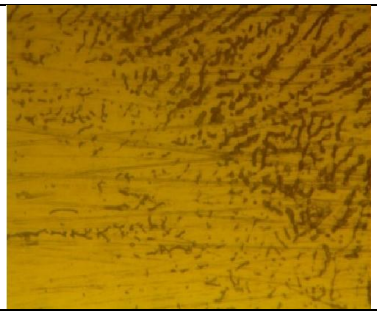
Experiment No. 4 Shielding Gas type = Ar, Flux used = TiO_2, Current = 125 A, Gas flow Rate = 10 L /min, Torch angle = 70°.		
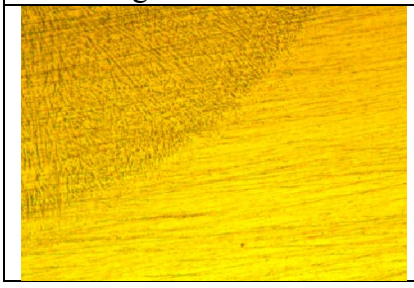	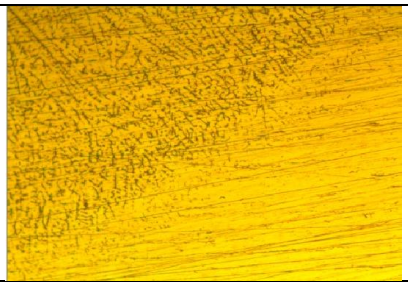	

Experiment No. 5
Shielding Gas type = Ar, Flux used = TiO_2, Current = 150 A, Gas flow Rate = 13 L /min, Torch angle = 90°.

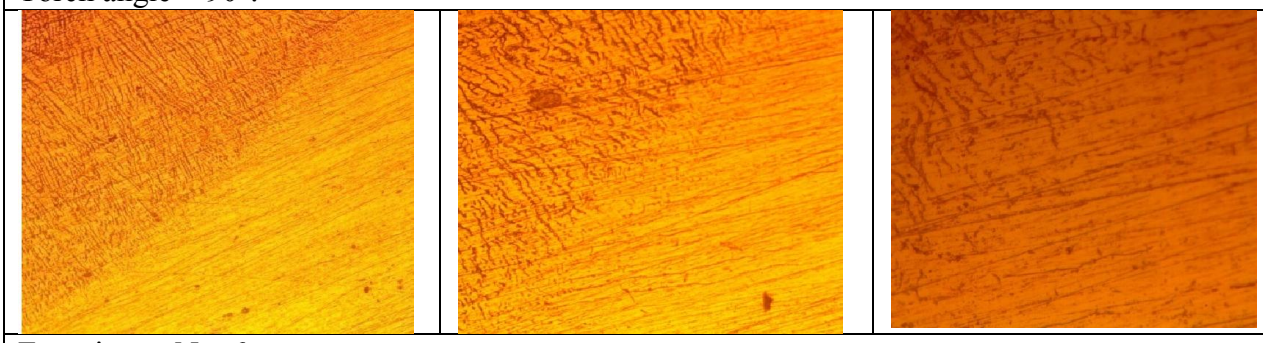

Experiment No. 6
Shielding Gas type = Ar, Flux used = TiO_2, Current = 175 A, Gas flow Rate = 16 L /min, Torch angle = 50°.

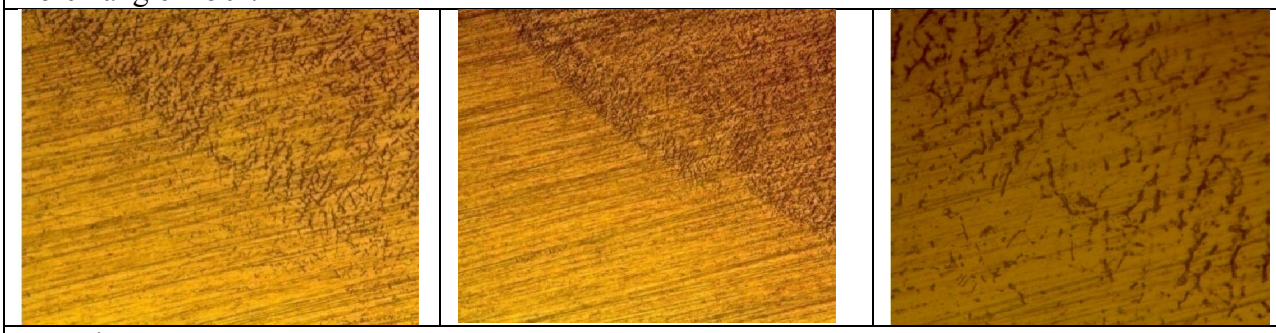

Experiment No. 7
Shielding Gas type = Ar, Flux used = MoS_2, Current = 125 A, Gas flow Rate = 13 L /min, Torch angle = 50°.

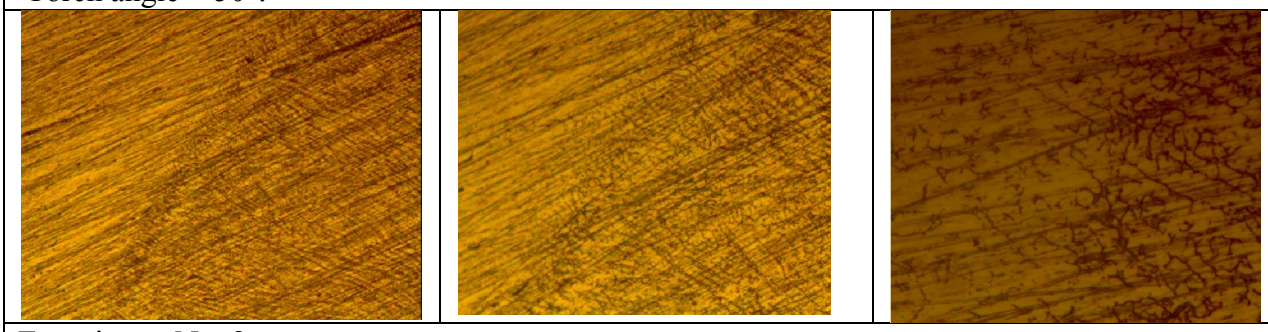

Experiment No. 8
Shielding Gas type = Ar, Flux used = MoS_2, Current = 150 A, Gas flow Rate = 16 L /min, Torch angle = 70°.

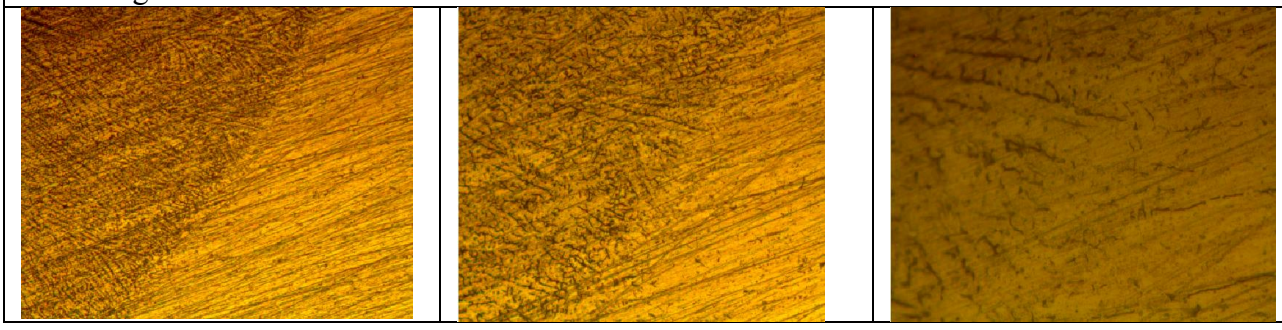

Experiment No. 9
Shielding Gas type = Ar, Flux used = MoS_2, Current = 175 A, Gas flow Rate = 10 L /min, Torch angle = 90°.

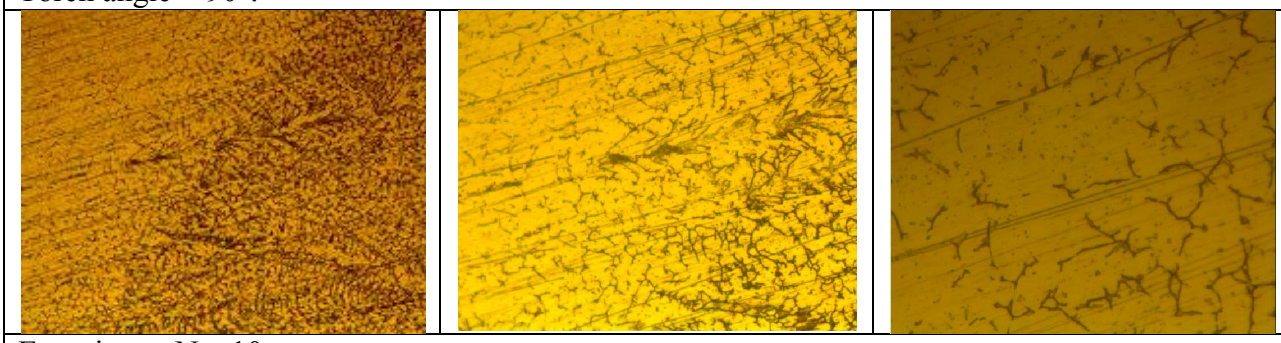

Experiment No. 10
Shielding Gas type = Ar+H_2, Flux used = SiO_2, Current = 125 A, Gas flow Rate = 16 L /min, Torch angle = 90°.

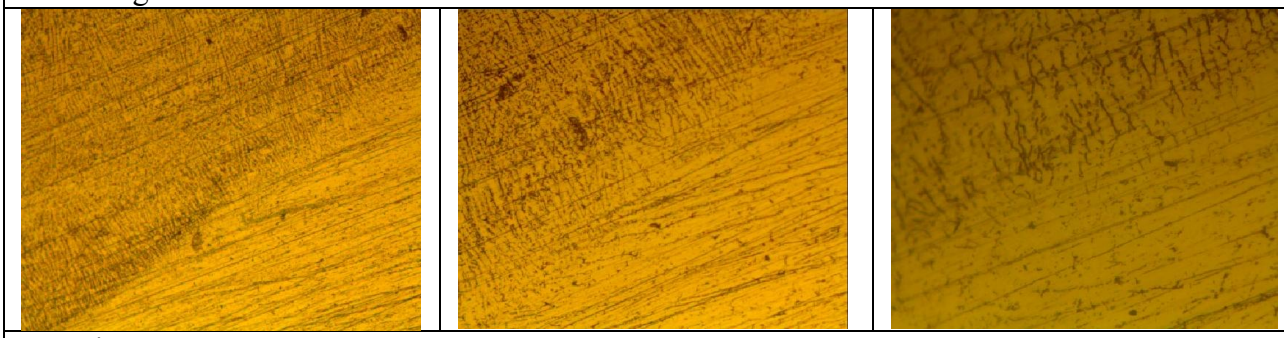

Experiment No. 11
Shielding Gas type = Ar+H_2, Flux used = SiO_2, Current = 150 A, Gas flow Rate = 10 L /min, Torch angle = 50°.

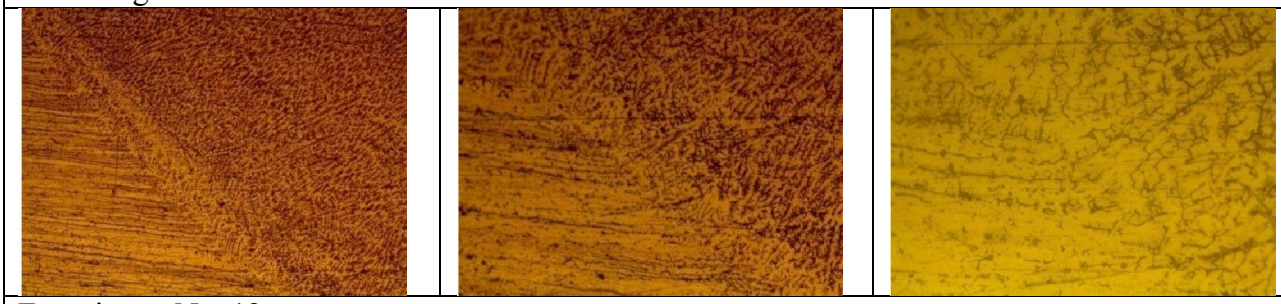

Experiment No. 12
Shielding Gas type = Ar+H_2, Flux used = SiO_2, Current = 175 A, Gas flow Rate = 13 L /min, Torch angle = 70°.

Experiment No. 13
Shielding Gas type = Ar+H_2, Flux used = TiO_2, Current = 125 A, Gas flow Rate = 13 L /min, Torch angle = 90°.

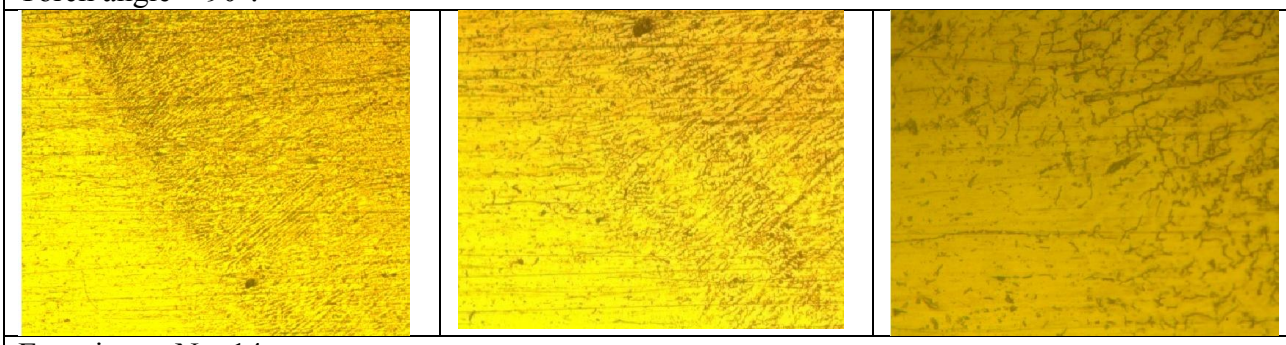

Experiment No. 14
Shielding Gas type = Ar+H_2, Flux used = TiO_2, Current = 150 A, Gas flow Rate = 16 L /min, Torch angle = 50°.

Experiment No. 15
Shielding Gas type = Ar+H_2, Flux used = TiO_2, Current = 175 A, Gas flow Rate = 10 L /min, Torch angle = 70°.

Experiment No. 16
Shielding Gas type = Ar+H_2, Flux used = MoS_2, Current = 125 A, Gas flow Rate = 16 L /min, Torch angle = 70°.

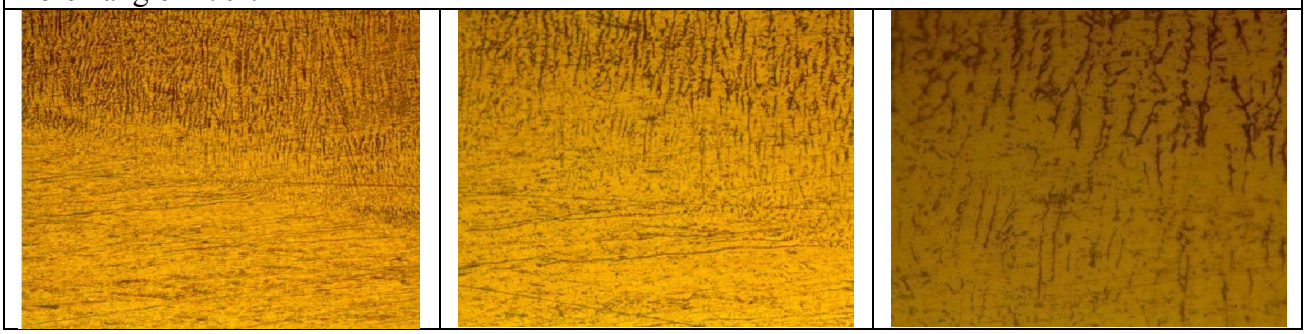

Experiment No. 17 Shielding Gas type = Ar+H_2, Flux used = MoS_2, Current = 150 A, Gas flow Rate = 10 L /min, Torch angle = 90°.
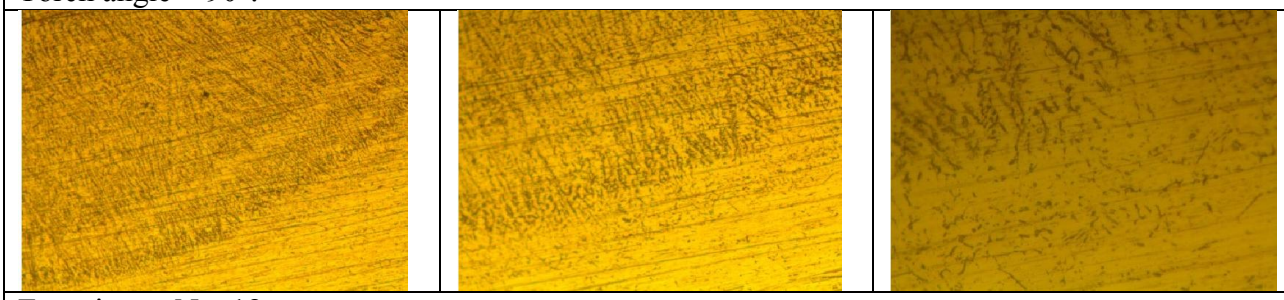
Experiment No. 18 Shielding Gas type = Ar+H_2, Flux used = MoS_2, Current = 175 A, Gas flow Rate = 13 L /min, Torch angle = 50°.


4.5.2 Metallurgical observation for Duplex 2205

For material Duplex 2205 etched with Carpenter etchant. The transformation of ferrite to austenite in the weld zone. Molten pool gets solidified from the liquid form to ferrite phase because of high content of ferrite stabilizers (chromium and molybdenum) in the material. As soon as the pool gets cool to room temperature transformation takes place from ferrite to austenite and looks like spots. Larger ferrite spots were found in different cases

Table 4.38: Microstructure of all the experiment of the Duplex 2205

Experiment No. 1 Shielding Gas type = Ar, Flux used = SiO_2, Current = 125 A, Gas flow Rate = 10 L /min, Torch angle = 50°.
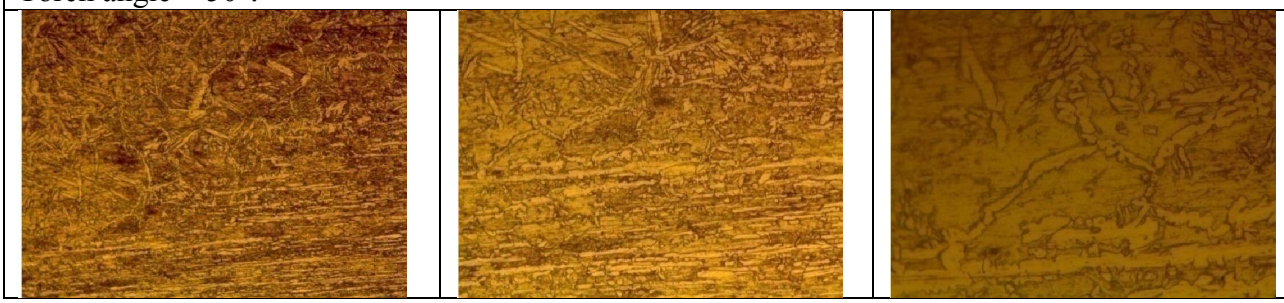

Experiment No. 2
Shielding Gas type = Ar, Flux used = SiO_2, Current = 150 A, Gas flow Rate = 13 L/min, Torch angle = 70°.

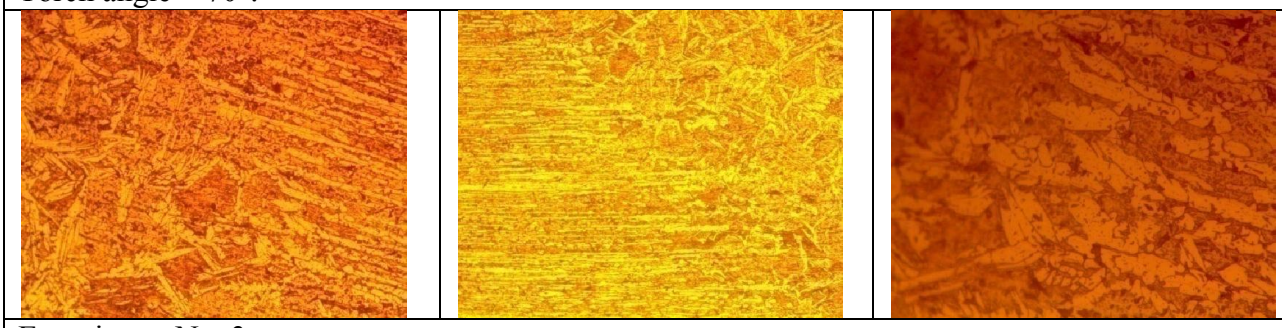

Experiment No. 3
Shielding Gas type = Ar, Flux used = SiO_2, Current = 175 A, Gas flow Rate = 16 L /min, Torch angle = 90°.

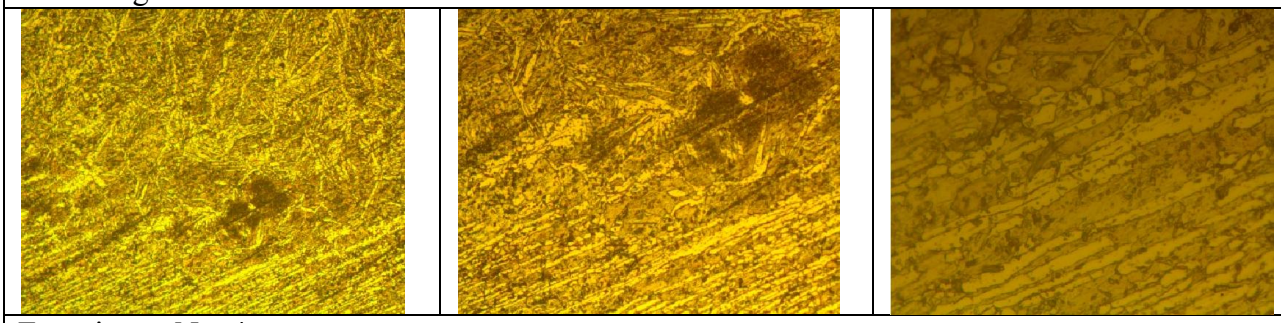

Experiment No. 4
Shielding Gas type = Ar, Flux used = TiO_2, Current = 125 A, Gas flow Rate = 10 L /min, Torch angle = 70°.

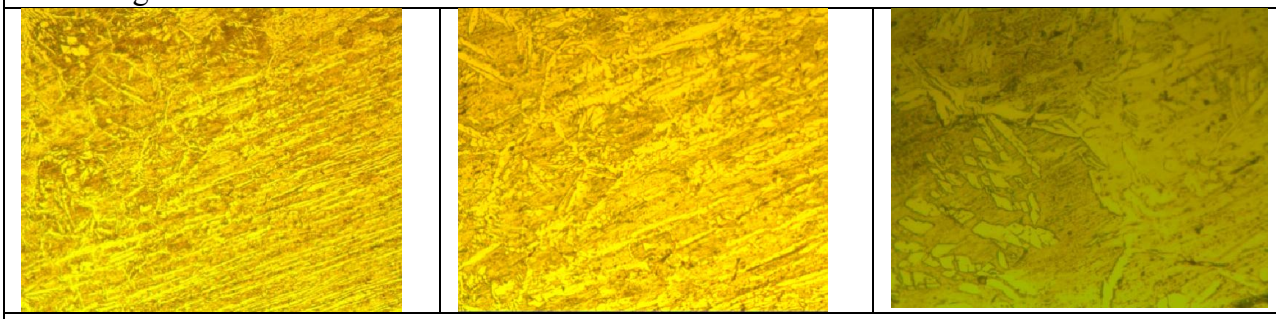

Experiment No. 5
Shielding Gas type = Ar, Flux used = TiO_2, Current = 150 A, Gas flow Rate = 13 L /min, Torch angle = 90°.

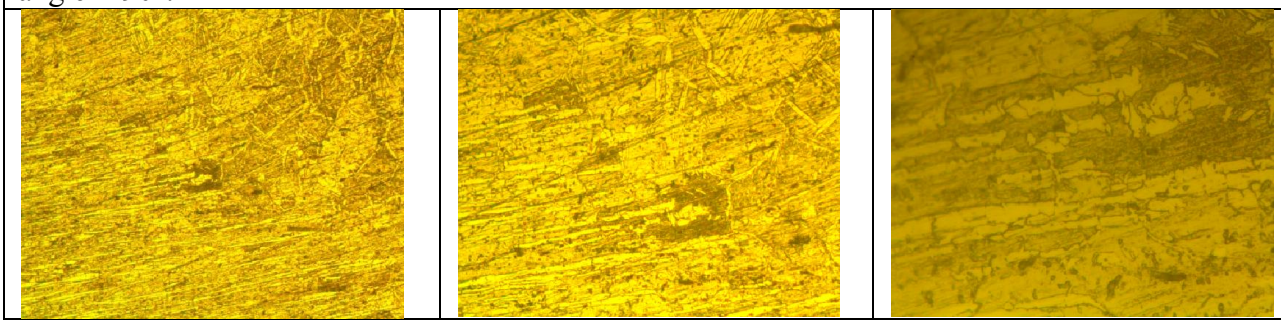

Experiment No. 6
Shielding Gas type = Ar, Flux used = TiO_2, Current = 175 A, Gas flow Rate = 16 L /min, Torch angle = 50°.

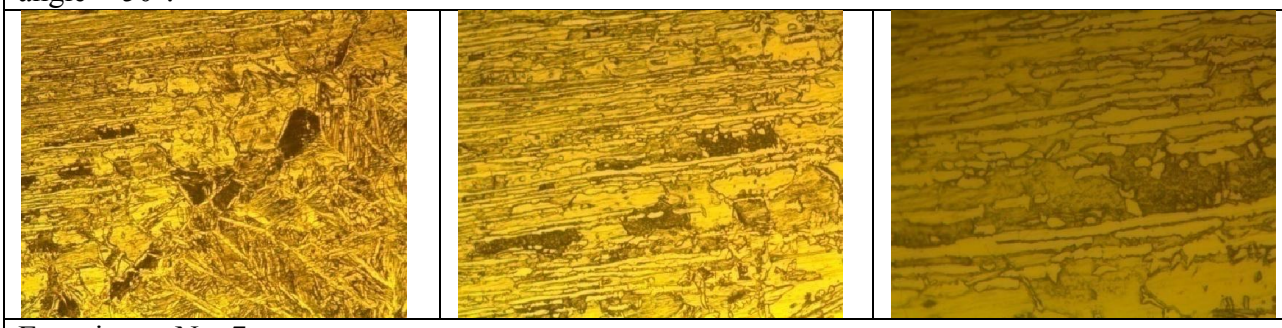

Experiment No. 7
Shielding Gas type = Ar, Flux used = MoS_2, Current = 125 A, Gas flow Rate = 13 L /min, Torch angle = 50°.

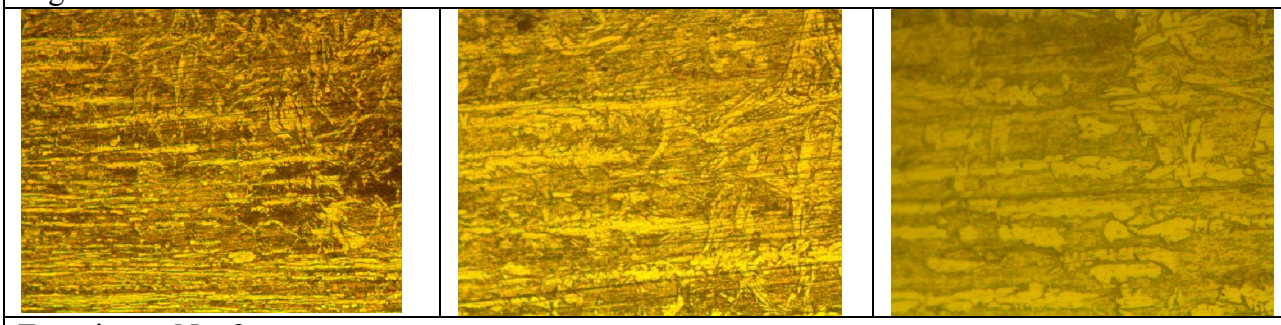

Experiment No. 8
Shielding Gas type = Ar, Flux used = MoS_2, Current = 150 A, Gas flow Rate = 16 L /min, Torch angle = 70°.

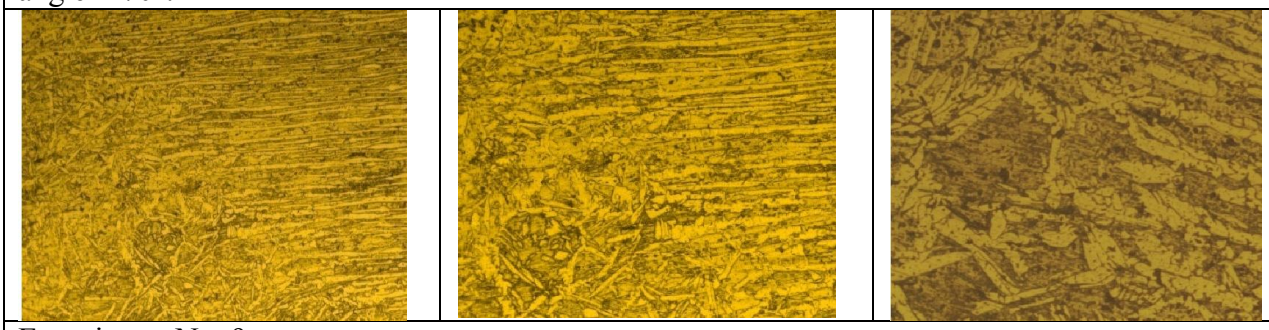

Experiment No. 9
Shielding Gas type = Ar, Flux used = MoS_2, Current = 175 A, Gas flow Rate = 10 L /min, Torch angle = 90°.

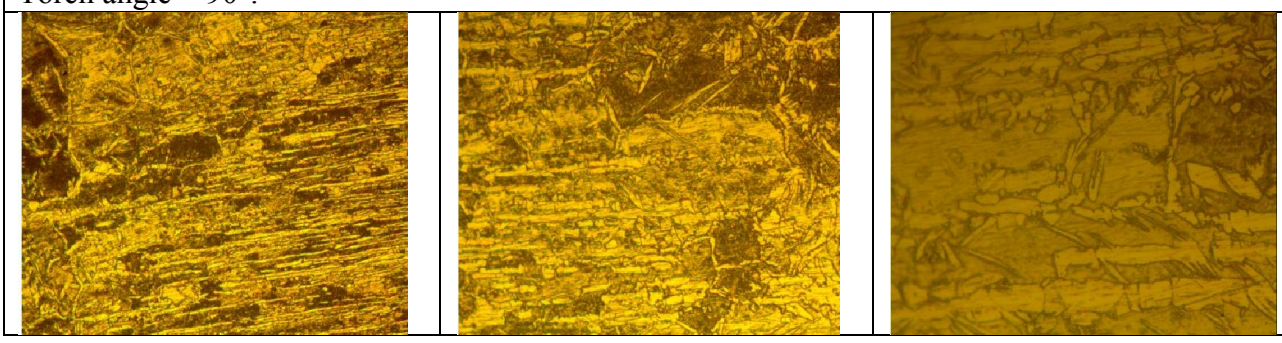

Experiment No. 10
Shielding Gas type = Ar+H_2, Flux used = SiO_2, Current = 125 A, Gas flow Rate = 16 L /min, Torch angle = 90°.

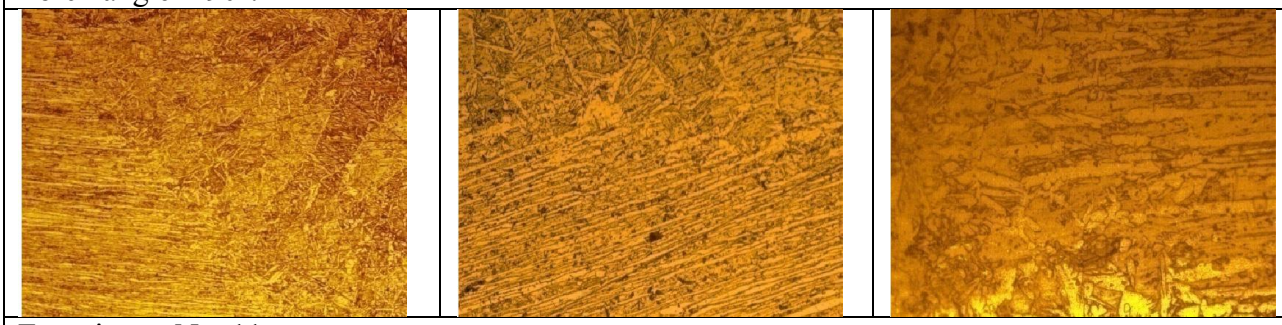

Experiment No. 11
Shielding Gas type = Ar+H_2, Flux used = SiO_2, Current = 150 A, Gas flow Rate = 10 L /min, Torch angle = 50°.

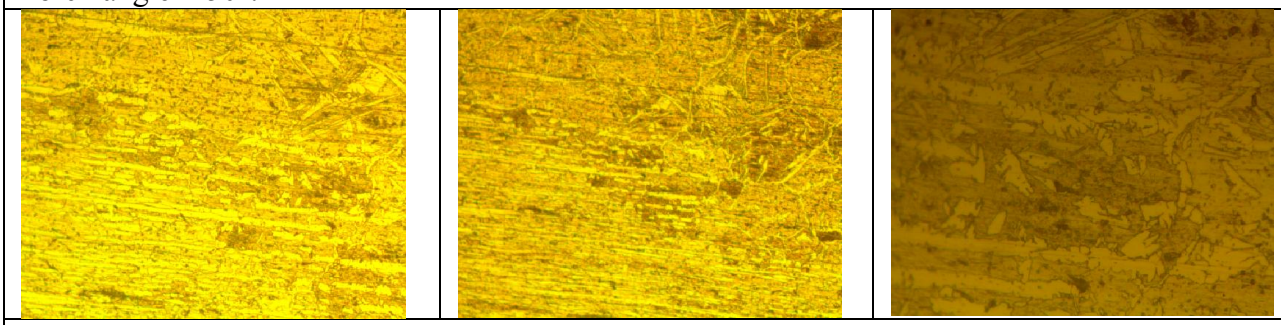

Experiment No. 12
Shielding Gas type = Ar+H_2, Flux used = SiO_2, Current = 175 A, Gas flow Rate = 13 L /min, Torch angle = 70°.

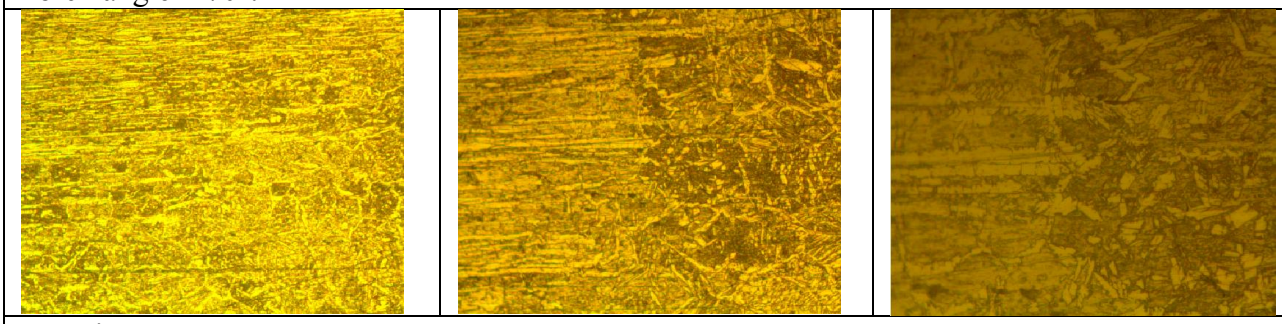

Experiment No. 13
Shielding Gas type = Ar+H_2, Flux used = TiO_2, Current = 125 A, Gas flow Rate = 13 L /min, Torch angle = 90°.

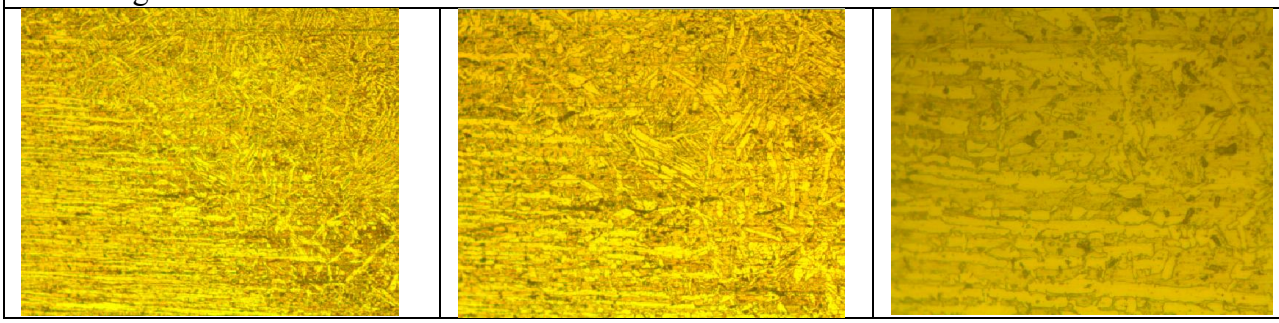

Experiment No. 14
Shielding Gas type = Ar+H_2, Flux used = TiO_2, Current = 150 A, Gas flow Rate = 16 L /min, Torch angle = 50°.

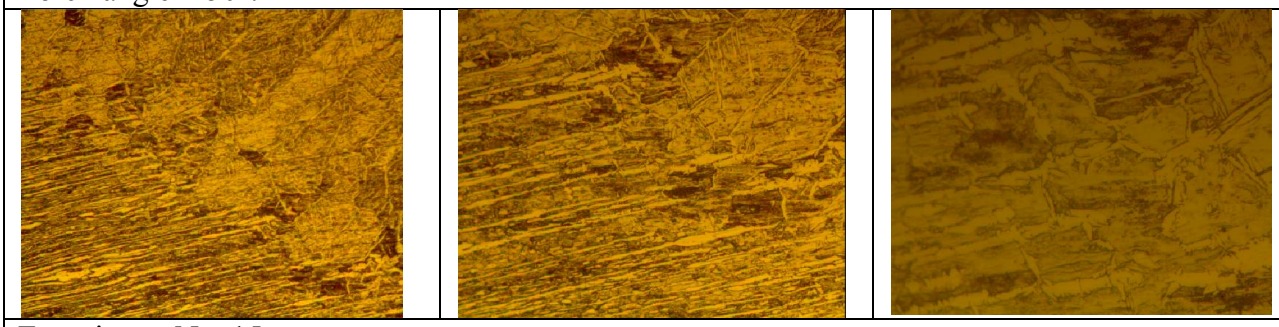

Experiment No. 15
Shielding Gas type = Ar+H_2, Flux used = TiO_2, Current = 175 A, Gas flow Rate = 10 L /min, Torch angle = 70°.

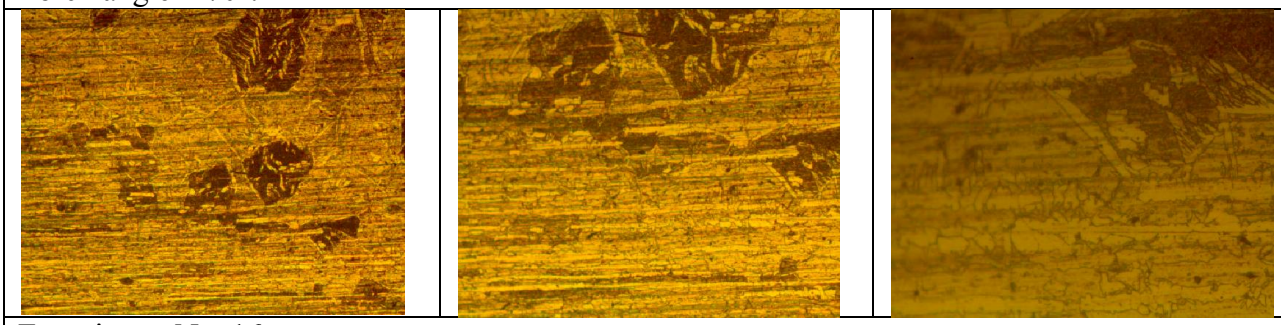

Experiment No. 16
Shielding Gas type = Ar+H_2, Flux used = MoS_2, Current = 125 A, Gas flow Rate = 16 L /min, Torch angle = 70°.

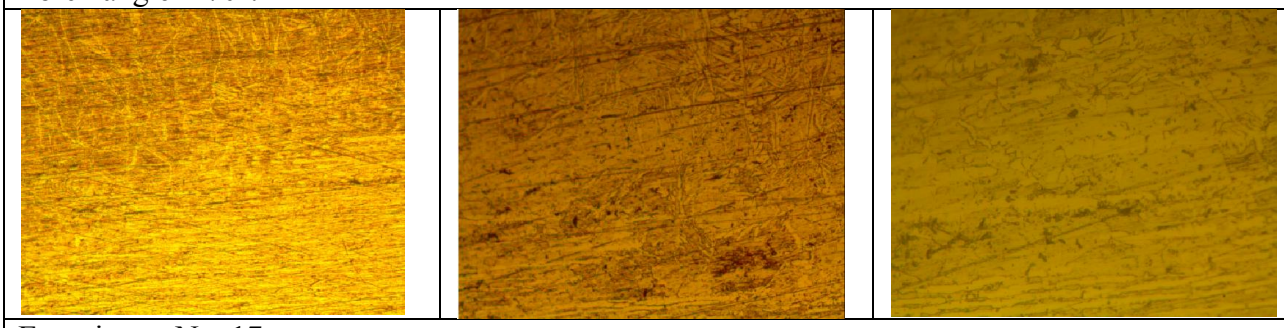

Experiment No. 17
Shielding Gas type = Ar+H_2, Flux used = MoS_2, Current = 150 A, Gas flow Rate = 10 L /min, Torch angle = 90°.

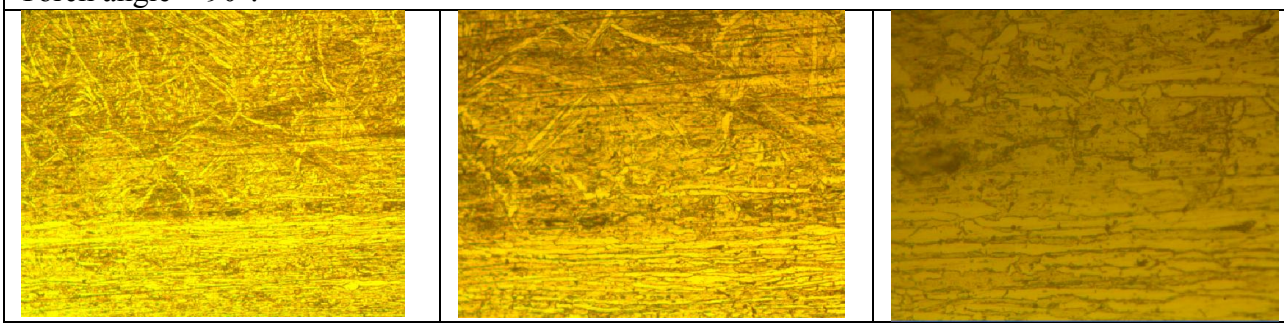

Experiment No. 18 Shielding Gas type = Ar+H_2, Flux used = MoS_2, Current = 175 A, Gas flow Rate = 13 L /min, Torch angle = 50°.		
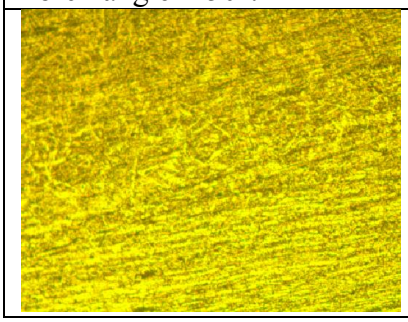	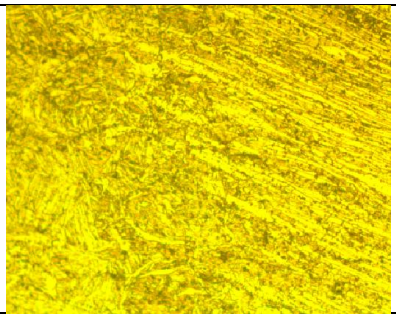	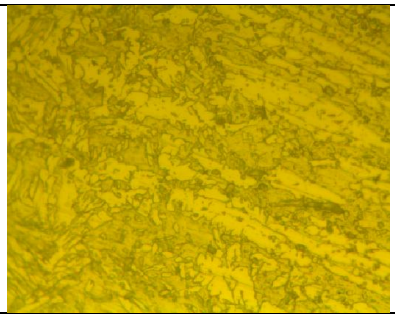

Chapter 5

Conclusions and Future Scope

5.1 Conclusions

In this study, the effect of different parameters on mechanical properties (bending, toughness) and variation in microhardenss were carried out during ATIG welding. The experiments were carried out for two different types of stainless steel namely Austenitic AISI 316 and duplex 2205 steel. Based on experimental results and subsequent statistical analsis, the following conclusions are drawn:

- During bending test, type of flux is found to be the most significant factor for both AISI 316 and Duplex 2205 steel. Maximum bending load can be carried out by welded joints using flux SiO_2. It is found that moderate torch angle helps to increase the bending load for AISI 316. In case of duplex 2205, minimal torch angle helps to improve the beding load. In both the cases, higher gas flow rates helps to improve the bending result. When effect of shielding gases are studied, $Ar+H_2$ increases the bending load. In case of current, minimal current causes higher bending load in AISI 316 but for Duplex 2205 higher current leads to higher bending load.
- During toughness test, pure Ar as sheilding gas is found to be increasing the toughness of the weld joint of AISI 316 but in case of Duplex 2205, $Ar+H_2$ is found to be increasing the toughness. H_2 may cause pores in the weld joint. Flux TiO_2 increases toughness for both the weld joints of both the materials. Higher current leads to higher toughness and lower gas flow rate increases toughness in AISI 316 and higher gas flow rate icreases tougness in Duplex 2205. In both the cases, lower torch angle increases the toughness.
- During microhardness test, pure argon is found to be increasing microhardness at fusion zone of AISI 316 and HAZ of Duplex 2205. On ther other side, $Ar+H_2$ is found to be increasing microhardness at HAZ of AISI 316 and Duplex 2205. Flux MoS_2 increased the microhardness at both the zones of AISI 316 in fusion zone of Duplex 2205 but in case of HAZ, SiO_2 increases the microhardness. Nominal level of current increases

microhardness at fusion zone of AISI 316. For HAZ, lower current increses microhardness. For Duplex 2205, optimum reason for the increament of microhardness is due to higher current. Nominal torch angle is found to be the reason behind higher microhardenss for AISI 316. For duplex 2205, higher current raises microhardness at HAZ and lower current raises microhardness at fusion zone. Nominal gas flow rate increases microhardness for both the material.

- During metallurgical observation, veins of ferrites are found in case of AISI 316 weld joint in HAZ. For Duplex 2205, ferritic spots are found in the interface of heat affcted zone and fusion zone.

5.2 Future scope

Following are the some future recommendations that can be carried out.

- Mixing shielding gas caused increase in mechanical properties for different kinds of steel. Different ratios of CO_2 into Ar can be used for TIG welding.
- Different kinds of flux can be mixed for more depth of penetration in TIG welding of AISI 316 Duplex 2205 if the thickness of the plates is more.
- The chemistry behind the mechanism of ATIG welding can be studied.
- Bending and reverse bending test can be carried out.
- Tensile test on the same study can be done.
- Effect of pre heat and post heat treatment can be studied.
- Optimum welding for thicker plates can be researched.
- Critical amount of flux to be applied for welding as more amount of flux causes poor results.

References

Arunkumar, V.; Vasudevan, M.; Maduraimuthu, V.; Muthupandi, V. (2012) Effect of Activated Flux on the Microstructure and Mechanical Properties of 9Cr-1Mo Steel Weld Joint. *Materials and Manufacturing Processes,* 27 (11): 1171—1177.

Chunli, Y.; Sanbao, L.I.N.; Fengyao, L.I.U.; Lin, W.U.; Qingtao, Z. (2003) Research on the mechanism of penetration increase by flux in ATIG welding. *J. Mater, SciTechnol,* 19(1): 225-227.

Chulin, D.; Yifeng, Z.; Guoming, C.; Hui, Z. (2004) Preliminary study on the mechanism of arc welding with the activating flux. *Aeronautical manufacturing technology, supplement* : 271-278.

Chern, T.S.; Tseng, K.H.; Tsai, H.L. (2011) Study of the characteristics of duplex stainless steel activated tungsten inert gas welds. *Material and Design,* 32: 255—263.

Devakumar, D.; Jabaraj, D. (2014) Research on Gas Tungsten Arc Welding of Stainless Steel – An Overview. *International Journal of Scientific & Engineering Research*, 1(5): 2229-5518

Dongjie, L.; Shanping, L.; Wenchao, D.; Dianzhong, L.; Yiyi, L. (2012) Study of the law between the weld pool shape variations with the welding parameters under two TIG processes. *Journal of Materials Processing Technology,* 212: 128—136.

Huang, H.; Shyu, S.W.; Tseng, K.H.; Chou, C.P. (2005) Evaluation of TIG flux welding on the characteristics of stainless steel. *Sci Techno Weld Join,* 10(5):566–73

Loureiro, A.R.; Costa, B.F.O.; Batista, A.C.; Rodrigues, A. (2009) Effect of activating flux and shielding gas on microstructure of TIG welds in austenitic stainless steel. *Science and Technology of Welding and Joining*,14(4):315-320.

Modenesi, P.J.; Eustaaquio, R.A.; Pereira, I.M. (2009) TIG welding with Single Component Fluxes. *Journal of Materials Processing Technology,* 99: 260-265.

Niagaj, J.; The use of activating fluxes for the welding of high-alloy steels by ATIG method. (2003)*Welding International,* 17(4):257–261.

Niagaj, J. (2011) Effect of ATIG welding on deformation of austenitic steel components. *Welding International,* 27(11): 853—856.

Patel, A.B.; Patel, S.P. (2014) The Effect of Activating Flux in TIG Welding. *International Journal of Computational Engineering Research,* 4: 65-70.

Rodrigues, A.; Loureiro, A. (2005) Effect of shielding gas and activating flux on weld bead geometry in tungsten inert gas welding of austenitic stainless steels. *Science and Technology of Welding and Joining,* 10(6): 760-765.

Shyu, S.W.; Huang, H.Y.; Tseng, K.H.; Chou, C.P. (2008) Study of the Performance of Stainless Steel ATIG Welds . *JMEPE,* 17: 193–201.

Tseng, K.H.; Hsu, C.Y. (2011) Performance of activated TIG process in austenitic stainless steel welds. *Journal of materials processing technolog,* 211: 503-312.

Tseng, K.H.; Li, P.Y. (2014) UNS S31603 Stainless Steel Tungsten Inert Gas Welds Made with Micro particle and Nanoparticle Oxides. *Materials,* 7:4755-4772.

Vasantharaja, P.; Vasundevan, M. (2012) Studies on ATIG welding of low activation ferritic/martensitic (LAFM) steel. *Journal of nuclear materials,* 421: 117-123.

Web References

W.1 The History of Welding. http://www.millerwelds.com/resources/articles/welding-history/. (accessed on - 03/07/2015).

W.2 Wikipedia. https://en.wikipedia.org/wiki/Gas_tungsten_arc_welding, (accessed on - 04/07/2015).

W.3 Marangoni flows. http://web.mit.edu/2.21/www/Lec-notes/Surfacetension/Lecture4.pdf , (accessed on - 06/07/2015).

Appendices

Curriculum vitae

Sneh Pragya is presently enrolled in Master of Engineering program in CAD/CAM Engineering under Department of Mechanical Engineering, Thapar University, Patiala. She graduated in 2012 from University of Pune in Production Engineering. Her area of research work for her ME thesis is Parametric Study on Flux Activated Tungsten Inert Gas Welding of AISI 316 and Duplex 2205 Steel.